Gnangara Sustainability Strategy

An across-government initiative

Groundwater – Biodiversity – Land use

MAPPING THE EXTENT AND RATE OF SPREAD OF *PHYTOPHTHORA CINNAMOMI* IN *BANKSIA* WOODLANDS ON THE GNANGARA GROUNDWATER SYSTEM

Katherine Zdunic, Janine Kinloch, Barbara Wilson and Leonie Valentine

Department of Environment and Conservation

April 2010

GOVERNMENT OF WESTERN AUSTRALIA

Department of Water
Department of Agriculture and Food WA
Department for Planning and Infrastructure
Department of Environment and Conservation

WATER CORPORATION

CSIRO

Forest Products Commission WESTERN AUSTRALIA

Mapping the Extent and Rate of Spread of *Phytophthora cinnamomi* in *Banksia* Woodlands on the Gnangara groundwater system

Report to the Department of Environment and Conservation and Gnangara Sustainability Strategy

Katherine Zdunic, Janine Kinloch, Barbara Wilson and Leonie Valentine

Department of Environment and Conservation

Government of Western Australia
Department of Environment and Conservation

Gnangara Sustainability Strategy Taskforce
Department of Water
168 St Georges Terrace
Perth Western Australia 6000
Telephone +61 8 6364 7600
Facsimile +61 8 6364 7601
www.gnangara.water.wa.gov.au

April 2010

Gnangara Sustainability Strategy

This document has been commissioned/produced as part of the Gnangara Sustainability Strategy (GSS). The GSS is a State Government initiative which aims to provide a framework for a whole of government approach to address land use and water planning issues associated with the Gnangara groundwater system. For more information go to www.gnangara.water.wa.gov.au

Acknowledgements
The Department of Environment and Conservation – Gnangara Sustainability Strategy would like to thank Dr Chris Dunne for reviewing this publication. Photo credits to Dr Leonie Valentine, images are of *Phytophthora cinnamomi* infested bushland.

Contents

Mapping the Extent and Rate of Spread of *Phytophthora cinnamomi* in *Banksia* Woodlands on the Gnangara groundwater system

Executive Summary

Phytophthora cinnamomi is a soil-borne water mould that is listed as one of the world's 100 most devastating invading species by the IUCN Species Survival Commission. The plant pathogen has been shown to alter plant species abundance and richness, as well as the structure of vegetation in sclerophyllous vegetation throughout Australia and *Phytophthora* dieback is listed as a 'key threatening process' in the Australian environment. The leached sands of the Swan coastal plain in Western Australia provide favourable conditions for the pathogen and its presence is often highly visible, with old diseased areas displaying reduced biomass and structural complexity. *Banksia* woodlands account for 50 % of the current extent of native vegetation on the Gnangara Groundwater System of the Swan coastal plain. They are of high conservation significance and the impact of *P. cinnamomi* is one of the major threatening processes affecting the woodlands.

Knowledge about the location of *P. cinnamomi* in the landscape is essential to determine management priorities and actions. Methods employed to map infestations, include on-ground surveys of symptoms, sampling for presence of the pathogen, and interpretation of disease symptoms using aerial photographs. However the methods are expensive and maps showing infestation boundaries have limited temporal currency due to continual spread of the pathogen. Remote sensing and image analysis methods are being increasingly adopted as tools for broad scale disease mapping and management and have advantages for monitoring vegetation dynamics over time.

This project sought to gain a greater understanding of how the application of remote sensing and geographic information system (GIS) technologies can be used to map the impact of *Phytophthora* dieback in *Banksia* woodlands and to investigate the current and historical rate of spread of the pathogen. The objectives were to: determine if Landsat Trend data can identify areas where vegetation has been impacted by *P. cinnamomi;* map changes in vegetation over time (1943 – 2008); assess the rate of spread of the pathogen,

and determine the influence of factors such as vegetation, soils, topography on the rate of spread.

The study was conducted at four study sites that were selected to include a range of topographical features and depths to ground water. At one of the sites (Warbrook Road) the earlier invasion of *P. cinnamomi* had been studied previously (Hill *et al.* 1994). The extent of impact of the disease was unknown at the other three sites (Pinjar, Neaves and Gnangara).

Mapping of *Phytophthora* dieback impact utilised a time series of orthophotos from 1953 to 2008. Aiding the identification of disease impact areas were Landsat Trend satellite imagery and Landsat Trend data, with capture dates between 1988 and 2008. Ground validation was undertaken by disease interpreters from the DEC Forest Management Branch. Linear measurement of disease rate of spread was undertaken in an area of very high quality mapping where the fronts for each time interval (epoch) were clear, and there was no evidence of other impacts such as fire, that may decrease the accuracy of mapping. Measurements were made between two adjacent fronts (approximately 10 year epochs) and the rate of spread was calculated per epoch as meters per year. The rate of spread was examined in relation to a number of landscape factors including elevation, depth to water, slope, aspect, change and direction of elevation, and change and direction of depth to water. GIS methods were used to extract landscape attributes along the linear measurements of disease movement. Single and multi factor ANOVA's were used to determine what landscape factors significantly affected rate of spread.

A combination of interpretation of orthophotos and Landsat Trend information was successful in identifying *P. cinnamomi* impacted areas in the Warbrook Road, Pinjar and Gnangara study areas. No *P. cinnamomi* impacted areas were identified in the Neaves study area, and this was consistent with the results of the ground-based surveys. There was a high degree of overlap between areas identified as impacted by the disease from ground based survey methods and remote sensing methods although the boundaries of disease impacted areas did not always align exactly. This is likely to be related to the ability of ground based methods to more effectively discriminate disease impact in all structural layers and on individual plants of the ground strata in the early stages of infestation.

Remote sensing methods, on the other hand, can only detect the disease once it has had a major impact on the vegetation particularly the upper structural layers.

Our remote sensing assessment showed that many initial infestations in the study area begin as small foci and take time, in some cases decades, to move through the landscape autonomously. However, because the areas are not subject to adequate quarantine or hygiene, vectoring of the pathogen continues its spread across the landscape. The identification of these initial small foci by remote sense methods provides the opportunity to initiate hygiene, treatment and quarantine management to contain or prevent progressive spread of the disease.

Our analysis Warbrook Road area found that there was a large increase in impacted area between 1974 and 1988 and that a number of new infections occurred in 1988. Several of the discrete disease fronts identified in 1988 have subsequently coalesced to form two long fronts in the study area. The area of infestation increased substantially from 14% (65 ha) to 47% (214 ha) over the 55 years. The rate of spread was significantly higher between 1953 and 1963 (1.286m/year) and the lowest rate was recorded between 1997 and 2008 (0.526m/year). The rates of spread are of the same order of magnitude as other studies on the coastal sandplains (Hill *et al.* 1994; Shearer *et al.* 2004; Shearer and Hill 1989), but much less than those recorded for downhill extension in Banksia woodland of 8 m/year (Podger 1968).

Disease impact spread was at a higher rate in *Banksia, Melaleuca* woodland vegetation compared to Low open *B. attenuata* woodland. The former vegetation occurs more in low lying areas associated with near surface water tables while the latter occurs more broadly from dune crest to low lying areas making some areas dryer and thus less conducive environment for the pathogen. The dune crest areas are also likely to be infested at a slower rate from upslope progression of the disease. A number of landscape factors were also found to have an impact on the rate of spread of the pathogen. The rate of spread of the pathogen was higher on soil types of humus podzols of poorly drained depressions, and areas subject to seasonal inundation where moisture levels are higher and therefore are more conducive to spread. Rate of spread was greater in areas which have a southern aspect and therefore are in shadow for greater periods of time, conditions also conducive to the pathogen. It was also higher in areas with low to mid elevation and areas where the groundwater is close to the surface, the two variables being not independent. The rate of spread of the pathogen was also higher in those areas of the landscape where elevation change was steep, regardless of direction, and the groundwater was moving either downgrade or upgrade.

There were significant interactions between epoch, vegetation type, depth to water, elevation change and slope direction. For example in the *Banksia, Melaleuca* woodland vegetation the pathogen was restricted to areas with near surface water early on (1953-63) and in later epochs was present in all depth to water categories. The restriction of the pathogen to more shallow depth to water categories in the early years is a reflection of the initial spread of the pathogen along the flank of the floodplain where depth to water was generally shallower.

While there were slow rates of spread on flat areas and fast rates of spread on steep uphill or downhill areas for the first three epochs (1953 – 1988) for both vegetation types, in the final epoch (1997 – 2008) the rate of spread was much lower and no trend with steepness was evident. Further while there was no consistent trend between vegetation type and slope direction in the early epochs (1953– 1988) subsequently the *Banksia, Melaleuca* vegetation type (J1) generally had a higher rate of spread across all slope directions.

Examination of rainfall patterns indicated that rainfall may be a major factor influencing the rate of spread. There was a higher rate of spread across all categories of tested landscape factors in those epochs experiencing higher winter rainfall (1953 – 1963, 1963 – 1974 and 1974 – 1988); and a slower rate of spread for the 1997 – 2008 epoch when average winter monthly rainfall declined. It is possible that rainfall has an over-riding influence on rate of spread and the influence of landscape variables such as slope, are less influential. Further analyses of rainfall impacts on rate of spread are required. These could include impacts of monthly, annual or winter rainfall on rates of spread within the epochs and any interactions with variables such as vegetation type and slope direction.

While there were some limitations to the current study, including in the use of remote sensing data, it has however greatly improved our assessment of the location of infestation and the rates of spread of *Phytophthora* dieback in *Banksia* woodlands, and provided information to better inform management of the pathogen on the GSS. Despite these limitations, the use of remote sensing technologies has a number of benefits. These include (1) the availability of orthophoto and Landsat image archives which enable historical and current mapping of disease impact to be undertaken; (2) can be applied over large areas thus allowing broad scale mapping to be undertaken; (3) no risk of spreading the disease whilst broad scale mapping is being undertaken. Therefore for organisations that have remote sensing capabilities these tools can provide a cost efficient way of identifying disease impact over broad scale areas of *Banksia* Woodlands. Once the extent of disease impact is known a risk assessment can be undertaken to prioritise and identify management actions such as more detailed on ground interpretation mapping or actions to protect biodiversity assets such as hygiene measures (if infested), quarantine measures (if un-infested) or phosphite application.

There were several recommendations for further investigation arising from the study. These included developing the model further by analysing rainfall impacts and developing regression models to resolve the most predictive factors continuing to apply remote sensing methods to monitor rates of spread of the pathogen and assess the efficacy of any management actions undertaken. Management recommendations included: the application and maintenance of hygiene standards for movement of vehicles along tracks; demarcation of tracks with standardized dieback posts; the upgrading or closing of tracks that intersect known infestations; the prioritisation of areas for the application of phosphite. Finally all management actions such as hygiene, quarantine measures, track closures, and application of phosphite can be evaluated by employing remote sensing techniques.

Introduction

The Gnangara groundwater system is located on the Swan Coastal Plain north of Perth and covers an area of approximately 2200 square kilometres. The groundwater system provides approximately 60% of Perth's drinking water (Government of Western Australia 2009). Declining ground water levels, climate change and increased abstraction have impacted the sustainability of the system and its significant ecological values (Government of Western Australia 2009). A multi-agency taskforce was established in 2007 to develop the Gnangara Sustainability Strategy (GSS) to assess land and water use policies, ecosystem assets and processes, and develop a decision making process to integrate values, risks and planning (DOW 2008). A major aim of the GSS is to address threats to regional conservation values.

Banksia woodlands account for 50 % of the current extent of native vegetation on the Gnangara groundwater system and their regional conservation significance is high. Clearing for urban and rural development across the Swan Coastal Plain has been to such an extent that very few large un-fragmented areas of remnant vegetation now exist, with the largest patch (68541 ha) south of the Moore River, occurring on the Gnangara groundwater system (GGS). Additionally some of the vegetation complexes occurring in this area do not have adequate levels of retention and protection (10-30% retained or protected) and some are only found within the Gnangara groundwater system (Kinloch *et al.* 2009a).

One of the threatening processes affecting the *Banksia* woodlands of the Gnangara groundwater system is the pathogen *Phytophthora cinnamomi*. Phytophthora dieback is listed as a 'key threatening process' in the Australian environment (Environment Australia 2009). Australian taxa that are highly susceptible to the pathogen include members of the Proteaceae family (e.g. *Banksia*), and the Papilionaceae and Myrtaceae families (e.g. *Eucalyptus marginata*, jarrah) (Shearer *et al.* 2007a). The leached sands of the Swan coastal plain provide favourable conditions for the pathogen (Shearer *et al.* 2007b). The presence of *Phytophthora* dieback is often highly visible, with old diseased areas typically displaying reduced biomass and structural complexity as a result of the removal of susceptible taxa.

Knowledge about the location of *P. cinnamomi* in the landscape is essential to determine management priorities and on-ground management actions (O'Gara *et al.* 2005). Methods employed to map the boundaries of infestations, including on-ground surveys of symptoms, soil sampling for presence of the pathogen, and interpretation of disease symptoms using aerial photographs (Bluett *et al.* 2003; Cahill *et al.* 2002; Daniel *et al.* 2006; Hogg and Weste 1975; O'Gara *et al.* 2005; Wilson *et al.* 1997). However, the detection, diagnosis and mapping of *P. cinnamomi* is expensive and maps showing *P. cinnamomi* infestation boundaries have limited temporal currency due to continual spread of the pathogen. There have been few systematic programs to map the extent of *P. cinnamomi* infestations in Australia. The collection of data, mainly by State Government departments has often been opportunistic or on a case-by-case basis.

Remote sensing and image analysis methods are being increasingly adopted as tools for broad scale disease mapping, assessment and management including forests and crops (Metternicht 2007; Nilsson 1995; Olsson *et al.* 2008; Ristaino and Gumpertz 2000). Satellite remote sensing technologies have advantages and are appropriate for monitoring vegetation dynamics over time.

This project sought to gain a greater understanding of how the application of remote sensing and geographic information system (GIS) technologies can be used to map the impact of Phytophthora dieback in *Banksia* woodlands and to investigate the current and historical rate of spread of the pathogen.

Specific objectives addressed:

1. Determine if Landsat Trend data can be used to identify areas where vegetation has been impacted by *Phytophthora cinnamomi* including in areas where limited field based information on the presence of the disease is available.
2. Map changes in the vegetation, related to the impact of *Phytophthora cinnamomi*, over several time periods using historical orthophotos.
3. Determine the rate of spread of *Phytophthora cinnamomi* over several time periods and determine what influence, if any, topographical or climate factors have on the autonomous rate of spread of the pathogen.

Background

The Pathogen

Phytophthora cinnamomi is a soil-borne water mould (Class Oomycetes) that is listed as one of the world's 100 most devastating invading species by the IUCN Species Survival Commission. The plant pathogen has been shown to alter plant species abundance and richness, as well as the structure of vegetation in sclerophyllous vegetation throughout Australia (McDougall *et al.* 2002b; Podger and Brown 1989; Shearer *et al.* 2007a; Weste 1974; Weste *et al.* 2002).

Factors essential for Phytophthora dieback to occur include the presence of the pathogen (*P. cinnamomi*) itself, susceptible plant hosts and favourable environmental conditions (e.g. warm, moist, infertile soils, poor drainage) (Cahill *et al.* 2008; Shearer *et al.* 2007a). Natural dispersion of *P. cinnamomi* occurs by growth through contacting root systems or by propagules in water flowing through surface and near-surface drainage systems (Shearer *et al.* 2007a). *P. cinnamomi* can be carried long distances in infested soil that is moved by human activities (Shearer *et al.* 2007a). Prominent Australian taxa that are susceptible include most of the Proteaceae family (e.g. *Banksia*), some of the Papilionaceae family, and a few of the Myrtaceae (e.g. *Eucalyptus marginata*, jarrah) (Shearer *et al.* 2007a). The leached sands of the Swan Coastal Plain provide favourable conditions for the pathogen (Shearer *et al.* 2007b).

The presence of Phytophthora dieback in a community is often highly visible, with old diseased areas typically displaying reduced biomass and structural complexity as a result of the removal of susceptible taxa. Areas where *P. cinnamomi* is active (the infection front) are identified by progressive stages of dead and dying vegetation (Shearer *et al.* 2007a). Observations of *P. cinnamomi* impact in south west Australia have shown the progression to be 0.7m to 2m a year (Grant and Barrett 2003; Hill *et al.* 1994; Shearer *et al.* 2004). Modification of vegetation structure and floristics associated with *P. cinnamomi* infestation has been linked to changes in small mammal communities, including reduced species richness and abundance of fauna in diseased vegetation, and decreased capture of individual species (Annett 2008; Laidlaw and Wilson 2006; Newell and Wilson 1993; Wilson 1990).

Mapping occurrence of *P. cinnamomi*

A number of methods have been employed to map the boundaries of infestations, including on-ground surveys of symptoms, soil sampling for presence of the pathogen, and interpretation of disease symptoms using aerial photographs (Bluett *et al.* 2003; Cahill *et al.* 2002; Daniel *et al.* 2006; Hogg and Weste 1975; O'Gara *et al.* 2005; Wilson *et al.* 1997). Some difficulties involved with mapping are evident. For example, the pathogen may be detected, but may not cause disease, or symptoms may not be visible due to the absence or low numbers of susceptible species. The useful life of maps of infestation boundaries is limited because of the natural rate of spread of the pathogen as well as the accelerated rate of spread of the pathogen under suitable conditions. Aerial photography is also considered ineffective for mapping in areas where the disease is restricted to understorey vegetation that is covered by a dense, *P. cinnamomi* resistant emergent layer.

Remote sensing and image analysis methods have been considered as suitable by organisations with remote sensing capacity, for addressing some of these concerns, and are being increasingly adopted as tools for broad scale disease mapping, assessment and management (Metternicht 2007; Nilsson 1995; Olsson *et al.* 2008; Ristaino and Gumpertz 2000). Examples include assessment of forest health (Chaerle and Van der Straeten 2000; Liu *et al.* 2006; Stone *et al.* 2001) and extent of crop disease (Apan *et al.* 2004; Lenthe *et al.* 2007; Mirik *et al.* 2006; Zhang *et al.* 2003). Satellite remote sensing technologies are appropriate for monitoring vegetation dynamics over time. They offer quantitative, repeatable methods using multi-date imagery that can be applied over large areas, and can be extended both retrospectively and into the future as data is captured on an ongoing basis (Furby *et al.* 2004; Pickup *et al.* 1993). Landsat satellite imagery, for example, has the spatial resolution and historical records that make it suitable for providing information for assessing change at scales ranging from small remnants to whole regions (Wallace *et al.* 2006).

An alternative to satellite imagery is remote sensing via airborne videography and airborne digital multi-spectral imagery (DMSI; Hill *et al.* 2009; Lamb 2000; Wallace *et al.* 2006; Wallace *et al.* 2007). Studies in *Banksia* woodlands on the Gnangara groundwater system have demonstrated that this method can detect changes at the level of individual trees

(Wallace *et al.* 2006; Wallace *et al.* 2007). A system for assessing *P. cinnamomi* related disease in the Bald Hills Heath in southern Victoria has also been successfully developed using this technique (Hill *et al.* 2009). Fine detail maps provided rapid availability of data that could be used for accurate measurement of the extent of disease and its changing status.

The impact of *Phytophthora cinnamomi* on Bassendean dune Banksia woodlands is characterised by a collapse of both the Banksia overstorey and a good proportion of the underlying shrub layer behind the disease front (Hill *et al.* 1994). This change in the vegetation can be easily detected in aerial photos by a marked increase in reflectivity and reduced levels of granularity (Hill *et al.* 1994). In other ecosystems methods to use orthophotos to map areas impacted by *Phytophthora* are well established (McDougall *et al.* 2002a). The change in vegetation, or more specifically the reduction in vegetation cover through time as disease front moves across the landscape, can also be detected by Landsat Trend Analysis (Furby *et al.* 2008) as a negative linear trend over the short to medium term.

In a previous study on the Gnangara groundwater system, Hill *et al.* (1994) successfully used historical aerial photographs (1953 – 1988) to map the location of disease fronts retrospectively, at a site on Warbrook Road, thus enabling information on disease progress patterns including rates of spread to be determined.

There are several studies using the presence/absence of *Phytophthora* impact areas to determine the physical landscape and climate conditions affecting the location of infection (Akashi and Mueller-Dombois 1995; Bluett *et al.* 2003; Wilson *et al.* 2003). A model of *P. cinnamomi* distribution at a local scale was developed for heathlands in the Anglesea district (Victoria), where GIS was employed to record site data, provide accurate estimation of spatial variables such as elevation, slope and contributing catchment area, and to develop a predictive spatial model for the distribution (Wilson *et al.* 2000; Wilson *et al.* 2003; Wilson *et al.* 1997). Logistic regression analysis of 17 variables (measured at sites and from the GIS attributes) identified two variables (elevation and sun-index) as statistically significant in determining the probability of *P. cinnamomi* infestation. The presence of infection was negatively associated with elevation (i.e. the lower the elevation, the more likely the presence of the pathogen) and positively associated with the sun-index (i.e. places that have a steep northerly aspect). These findings are consistent with the downhill spread of zoospores with free water movement and suggest that within the mid elevations of the catchment, the warmth associated with northerly aspects is conducive to *P. cinnamomi* activity. A spatial model was developed to assess correlations between *P. cinnamomi* disease and site characteristics in the Wet Tropics World Heritage Area (S. Worboys pers. comm; Gadek *et al.* 2001). The project was undertaken to determine if outbreaks of disease are associated with particular site characteristics, as although the pathogen is uniformly distributed in the area, disease expression does not always occur. Areas of disease were found to be correlated with acid–igneous geology, flat areas where drainage is impeded, notophyll dominant vegetation and elevations of 750 m and higher (Gadek *et al.* 2001).

The main limitation of these models is that they contains no dynamic elements (Austin 2002). Extrapolation from this type of static spatial model could be improved by considering the dynamics of the driving variables and feedback processes of the pathogen and the environmental and landscape factors at the sites.

Phytophthora dieback front movement

The documentation of measurement techniques and analysis of the progressive movement or growth of *Phytophthora* impact areas has not been extensive. On- ground measurement using evenly spaced rows of posts has commonly been employed and provides a rigorous method of disease movement over time (M. Grant pers. comm.). However this method is arduous over large areas, and introduces the risk of spreading the pathogen. The determination of disease impact movement through the landscape has been carried out utilising a time series of 'analogue stereo aerial photographs' by Hill *et al.* (1994). In this approach hand drawn front and manual measurement methods are utilised (Hill *et al.* 1994). The application of GIS tools to determine front movement appears to be less common. Some examples are the application of spatial autocorrelation techniques to examine the distribution of disease impacts at different time periods since first infection (Ristaino and Gumpertz 2000); comparisons of areal extent change in invasive species have also been carried out utilising remote sensing and GIS (Essa *et al.* 2006).

The rate of natural spread of the pathogen is strongly influenced by topography, vegetation and climate. Annual rates of spread are highly variable, ranging from several metres to hundreds of metres downslope in gullies or watercourses. In Western Australia, upslope disease extension on the Darling Plateau is 0.37 m/year, compared to 2.15 m/year for the Blackwood Sedimentary Plateau where a perched watertable provides long periods of favourable conditions for proliferation of the pathogen (Strelein *et al.* 2006). In the jarrah forest, upslope and across slope spread seldom exceeds an average of 1 m per year (Podger et al. 1996 cited in O'Gara *et al.* 2005). Rates of 0.7- 2m / year have been recorded in the Southern west Botanical province of Western Australia depending on climate, site and susceptibility of vegetation (Grant and Barrett 2003; Hill *et al.* 1994; Shearer *et al.* 2004). These rates are much less than those recorded for downhill extension in Banksia woodland of 8 m/year (Podger 1968), or 400 m / year in sands with an impeding horizon at 1- 8m depth at Wilson's Promontory in Victoria (Weste and Law 1973).

Methods and Datasets used

Study Area and Climate

The Gnangara groundwater system is located on the Swan Coastal Plain just north of Perth and covers an area of approximately 2200 square kilometres. It extends from the Swan River in the south, Moore River and Gingin Brook in the North and from Ellen Brook and Swan Valley in the east to the Indian Ocean to the West. The area has undergone intensive urban, rural and pine plantation development though extensive areas of Banksia Woodlands remain, as do permanent and seasonal wetlands. The groundwater system comprises several different hydrological units or aquifers and provides approximately 60% of Perth's drinking water (Government of Western Australia 2009). Declining ground water levels since the mid 1970s, climate change, increased abstraction and interception loss has brought into question the sustainability of the Gnangara groundwater system and its associated values (Government of Western Australia 2009).

The vegetation of the Gnangara groundwater system is dominated by heath and/or tuart woodlands on limestone, Banksia and jarrah – Banksia woodlands on dune systems of various ages, marri on colluvial and alluvial soils, and paperbarks in swampy areas (Mitchell *et al.* 2003). Mattiske (2003) identified 32 vegetation types on the Gnangara groundwater system based on available floristic plot data and the system developed by Havel (1968). This study focused on four vegetation types including two dryland vegetation types (G1 and I1) in which *Banksia attenuata* is the dominant species, and one wetland vegetation type (K1) in which *Eucalyptus rudis* subsp. *rudis* is the dominant species. The fourth vegetation type (J1) is a terrestrialising wetland in which *Corymbia calophylla* and *Banksia attenuata* are the dominant species. See Appendix A for a full description of vegetation types.

The Gnangara Mound experiences long dry summers and mild wet winters with 80% of its average annual rainfall falling between May and October (Government of Western Australia 2009). The long term average annual rainfall of the Perth Airport is 780 mm (1945 – 2007) but since the 1970's the wider south-west region has been experiencing a decline in rainfall with the annual average rainfall at Perth Airport declining to 727 mm post 1976 (datasource: Bureau of Meteorology; Government of Western Australia 2009).

Not only has the total amount of rainfall over a year declined so has the frequency of wet months with the number of months, per decade, with total rainfall greater than 150mm or 200mm declining since the 1970's (Government of Western Australia 2009).

Four study sites were selected in Banksia woodlands of the GGS. The sites were selected to include a range of topographical features and depths to ground water (Table 1 and Figure 1). One of the sites (Warbrook Road) had also been the site of a previous study of the invasion of *Phytophthora* (Hill et al. 1994). This site was included in the current study so as to provide an update on disease progress patterns on an area that had been infested for many years (since at least 1942). The extent of impact of the disease was unknown at the other three sites (Pinjar, Neaves and Gnangara). These sites where chosen as the presence of the disease had been confirmed by a positive sample (DEC Vegetation Health Service - VHS) or from anecdotal information from experienced colleagues who had visited sites recently and as these areas were part of a concurrent GSS project of on-ground *Phytophthora* surveys undertaken by a qualified dieback interpreter.

Table 1: Broad site descriptors of study sites. A full description of vegetation types and soil types are provided in Appendix A and Appendix B.

Area	**Elevation broad category (AHD)**	**Depth to water broad category (2005)**	**Major Soil Types (DAFWA Mapping Unit)**	**Major Vegetation Codes (Mattiske)**	**Presence of disease**
Pinjar	Average: 72m Range: 60 - 108m	Average: 15m Range: 4 - 52m	31% - 212Bs_Jas 28% - 212Bs_G 25% - 212Bs_Ja	33% - I1 33% - J1 20% - G1	2 positive VHS samples Observed in field 18/11/2008
Neaves	Average: 72m Range: 66 - 81m	Average: 5m Range: 0 - 16m	72% - 212Bs_Ja 14% - 212Bs_J 9% - 212Bs_Ws	53% - I1 39% - J1 7% - K1	1 positive VHS sample
Gnangara	Average: 67m Range: 55 - 82m	Average: 9m Range: 2 - 24m	67% - 212Bs_Ja 8% - 212Bs_G 7% - 212Bs_J	44% - J1 39% - I1 8% - K1	Small impact areas observed in field 2008
Warbrook Road	Average: 61m Range: 52 - 84m	Average: 8m Range: 1 - 37m	59% - 212Bs_Ja 15% - 212Bs_J 7% - 213Ya_8x 6.39% - 212Bs_G	54% - J1 27% - I1 7% - K1	Present since at least 1942, interpreted by DEC Forest Management Branch in 2008

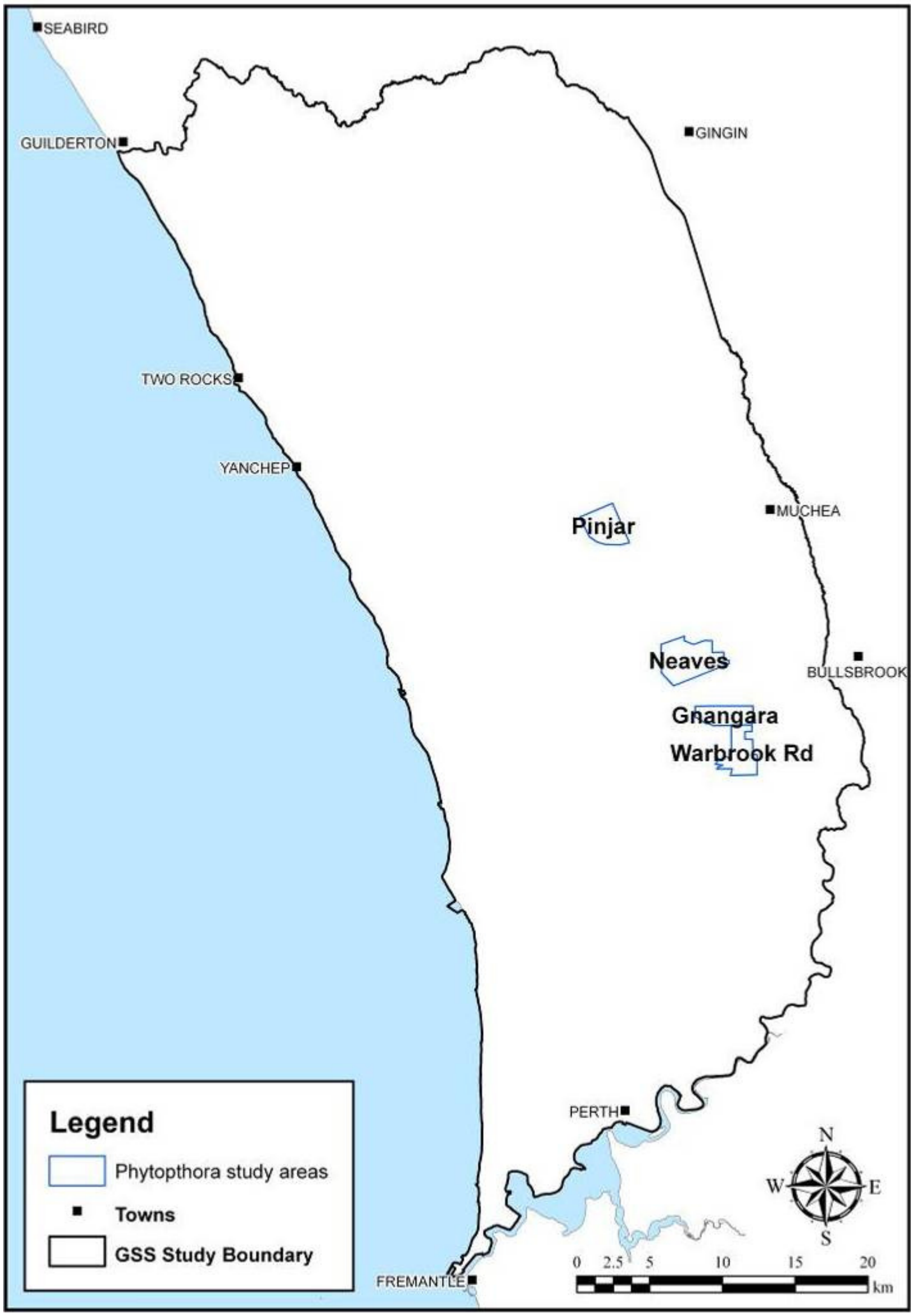

Figure 1: *Phytophthora* study sites location.

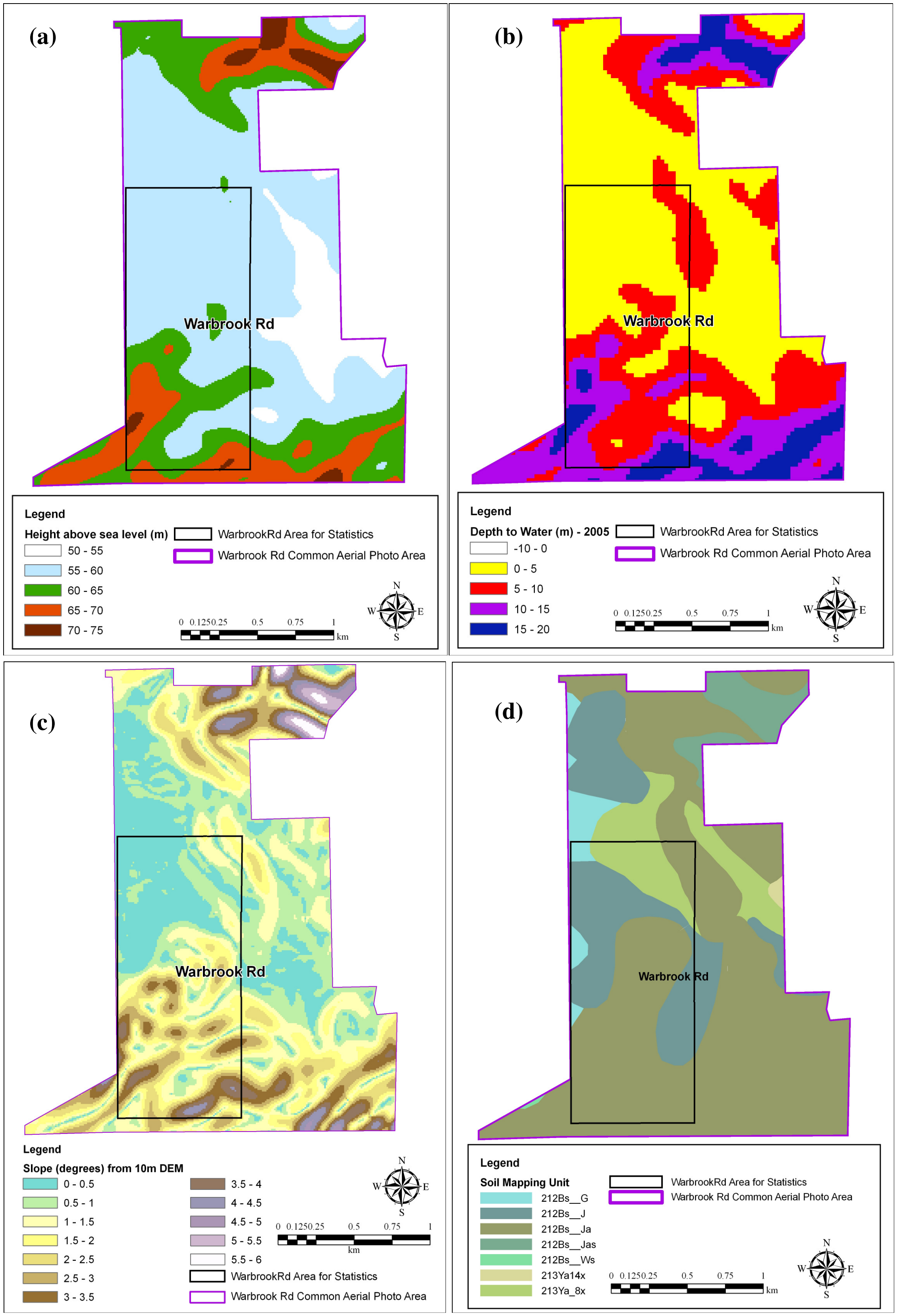
(a)
Warbrook Rd
Legend
Height above sea level (m)
50 - 55
55 - 60
60 - 65
65 - 70
70 - 75
WarbrookRd Area for Statistics
Warbrook Rd Common Aerial Photo Area
0 0.125 0.25 0.5 0.75 1 km
N S E W
(b)
Warbrook Rd
Legend
Depth to Water (m) - 2005
-10 - 0
0 - 5
5 - 10
10 - 15
15 - 20
WarbrookRd Area for Statistics
Warbrook Rd Common Aerial Photo Area
0 0.125 0.25 0.5 0.75 1 km
N S E W
(c)
Warbrook Rd
Legend
Slope (degrees) from 10m DEM
0 - 0.5
0.5 - 1
1 - 1.5
1.5 - 2
2 - 2.5
2.5 - 3
3 - 3.5
3.5 - 4
4 - 4.5
4.5 - 5
5 - 5.5
5.5 - 6
WarbrookRd Area for Statistics
Warbrook Rd Common Aerial Photo Area
0 0.125 0.25 0.5 0.75 1 km
N S E W
(d)
Warbrook Rd
Legend
Soil Mapping Unit
212Bs__G
212Bs__J
212Bs__Ja
212Bs__Jas
212Bs__Ws
213Ya14x
213Ya_8x
WarbrookRd Area for Statistics
Warbrook Rd Common Aerial Photo Area
0 0.125 0.25 0.5 0.75 1 km
N S E W

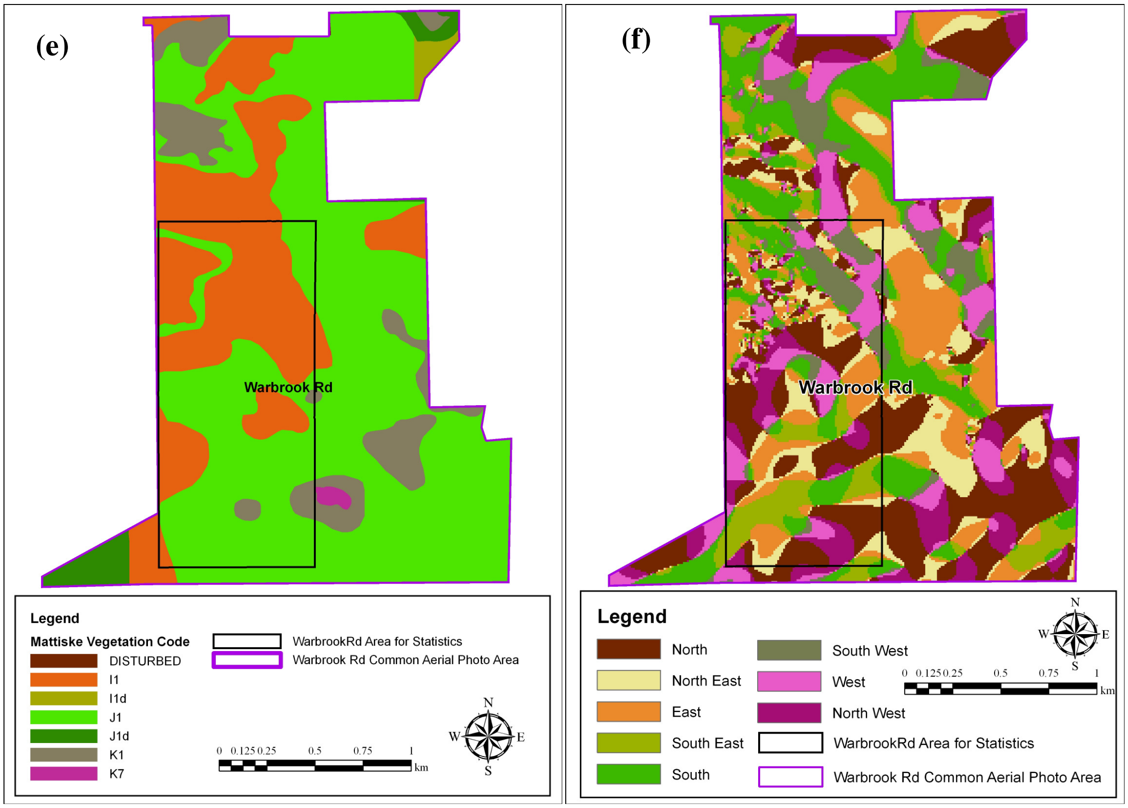

Figure 2: Distribution of landscape attributes across Warbrook Road site, (a): height above sea level, (b): depth to water, (c): slope, (d): soil map unit, (e): vegetation type, (f): aspect.

Datasets

The spatial data utilised in the mapping of the *Phytophthora* dieback impact included an extended time series of orthophotos (1953 to 2008) (Table 2). Aiding the identification of disease impact areas were enhancements and trend images created from Landsat 5 Thematic Mapper (TM) and Landsat 7 Enhanced Thematic Mapper Plus (ETM+) satellite imagery, with capture dates between 1988 and 2008 (Table 3). The satellite data was obtained with rectification and calibration corrections applied from the Land Monitor Project (Caccetta *et al.* 2000, http://www.landmonitor.wa.gov.au/)

Spatial datasets representing the landscape attributes at the Warbrook Road site included vegetation type, soil units, depth to ground water in 2005 and elevation (Table 4). The distribution of the landscape attributes across the Warbrook Road site are shown in Figure 2.

Climate data including daily rainfall, maximum and minimum temperatures are available for many stations irregularly spaced across the Gnangara Mound. Station 9029 located at Muchea Tree Farm provided the most consistent long range measurements back to 1953, this data was sourced from SILO (http://www.nrw.qld.gov.au/silo/).

Table 2: Dates of orthophotos used to digitise *Phytophthora* impact areas.

Orthophoto Date	Epoch	Epoch Length (years)
15/12/1953		
03/04/1963	1953-1963	9.3
10/07/1974	1963-1974	9.8
05/04/1987	1974-1987	12.8
15/12/1992	1987-1992	5.8
05/01/1997	1992-1997	4.0
Jan-2003	1997-2003	6.0
Jan-2008	2003-2008	5.0

Table 3: Dates of Satellite imagery used. Major scene date refers to the Landsat scene that covers the majority of the GSS area.

Epoch	Land Monitor Scene Date		Landsat Sensor	Pixel Size (m)
	Major	Minor		
1988	20/02/1988	NA	TM	25
1990	25/02/1990	14/12/1989	TM	25
1992	30/01/1992	NA	TM	25
1994	25/12/1993	19/01/1994	TM	25
1996	01/02/1996	25/01/1996	TM	25
1998	29/12/1997	NA	TM	25
2000	20/02/2000	NA	ETM+	25
2002	16/12/2001	09/02/2002	ETM+	25
2003	17/01/2003	NA	TM	25
2004	23/02/2004	NA	TM	25
2005	02/02/2005	09/02/2005	TM	25
2006	05/02/2006	12/02/2006	TM	25
2007	07/01/2007	14/01/2007	TM	25
2008	17/01/2008	NA	TM	25

Table 4: Spatial datasets representing landscape attributes at the Warbrook Road site.

Name	Description	Resolution	Data Type	Currency
Vegetation Types	Vegetation community mapping by Mattiske Consulting		Categorical vectors	2003
Soils	Soil landscape mapping by Department of Agriculture and Food		Categorical vectors	
Depth to Ground Water (DTW)	Modelled depth to groundwater by Department of Water	10m pixel	Continuous raster	2005 only
Digital Elevation Model (DEM)	Modelled digital elevation model by CSIRO Mathematical and Information Sciences	10m pixel	Continuous raster	2005

Mapping the Extent of Impact using Orthophotos and Landsat Trend Imagery

Current Extent of Impact

A combination of orthophotos and Landsat Trend information were used to initially identify suitable locations where *Phytophthora* dieback impact could be identified. At the Warbrook Road site, locations not identified in the previous study (Hill *et al.* 1994) as being impacted by the disease were also identified. The extent of the impact areas were then mapped at the scale of 1:5000 using 2008 orthophotos (captured at 1:20,000). Impact areas are defined as areas of changed vegetation structure where the change is not due to fire or grazing. To assist in determining the source of change to vegetation structure, we used Landsat derived vegetation trend images, which display the vegetation cover changes over time. The trend images thus assist in differentiating the movement of a *Phytophthora* front through the landscape which is more gradual, from abrupt changes in vegetation caused by disturbance such as fire or grazing (Figure 3).

Ground validation was then undertaken by comparing the extent of the areas mapped using these methods with the spatial information captured as part of on-ground surveys of the Gnangara, Neaves and Warbrook Road areas by the DEC Forest Management Branch. The Pinjar site was not part of the on-ground surveys for the GSS so field validation could not be as extensive and only a sample of the areas identified, remotely, as being impacted by the disease were visited.

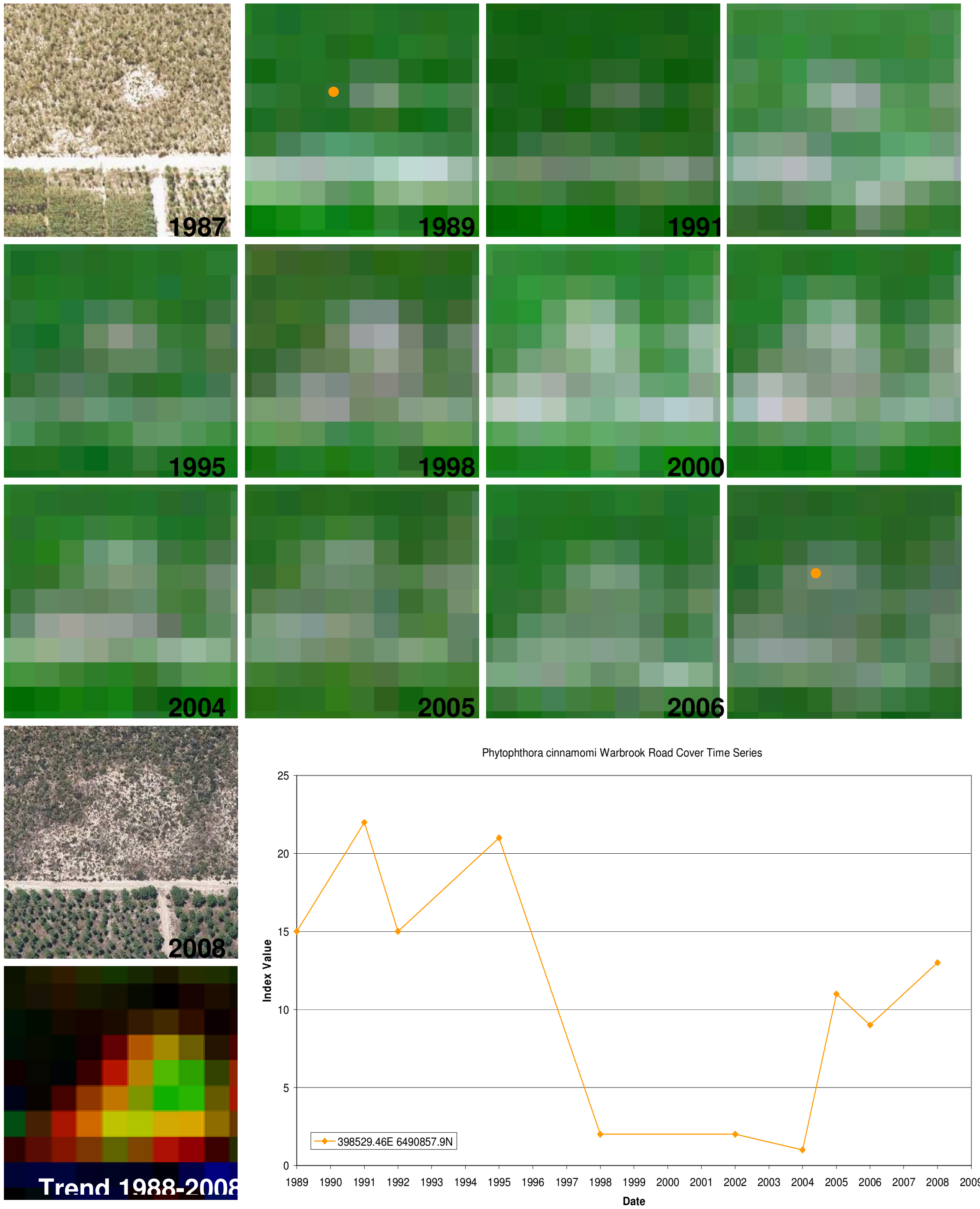

Figure 3: Impact of *Phytophthora cinnamomi* on a 25m Landsat 5 TM pixel. Top left 1987 aerial photo, following 11 images left to right are AGO Landsat images bands 3, 4 and 2 shown in red green and blue respectively, bottom left 2008 aerial photograph and Landsat trend image using dates 1988-2008 red is vegetation cover loss blue is gain and green is variation, bottom right graph of a single pixel's Projective Foliage Cover (PFC) values in the Landsat 5 TM sequence.

Historical Extent of Impact

The on-ground validation agreed with the 2008 mapping from orthophotos and Landsat trend information. With this knowledge the capture of *Phytophthora* impact areas at the Warbrook Road site continued utilising orthophotos specified in Table 2. The boundaries of impact areas at some locations for some dates were not clear as vegetation cover can at times be also affected by other natural (eg., fire) or non-natural (eg., clearing or grazing) processes. This affect was mitigated by not digitising an impact when the change was obviously not caused by *Phytophthora*, and assigned a rating of quality to the digitised areas. Due to the scale of the photographs the movement of the *Phytophthora* impacted area needs to be at least a few meters to effectively map between dates. For this reason the photograph capture dates need to be at least five years apart, preferably ten years.

The observations used to calculate the measures of disease impact at Warbrook Road were derived from two study areas (Figure 4). The area statistics were calculated from digitised fronts within the common area of all the orthophotos (purple line in Figure 4) and encompassing both areas that were infected in 1953, and areas not infected at this time. This provided a broader assessment of expansion of disease impact area and how the disease progressed with time. Linear measurement of disease rate of spread was undertaken in the area of very high quality mapping (black line in Figure 4) where the fronts over the total time were clear, and there was no evidence of other impacts such as fire, that may decrease the accuracy of mapping.

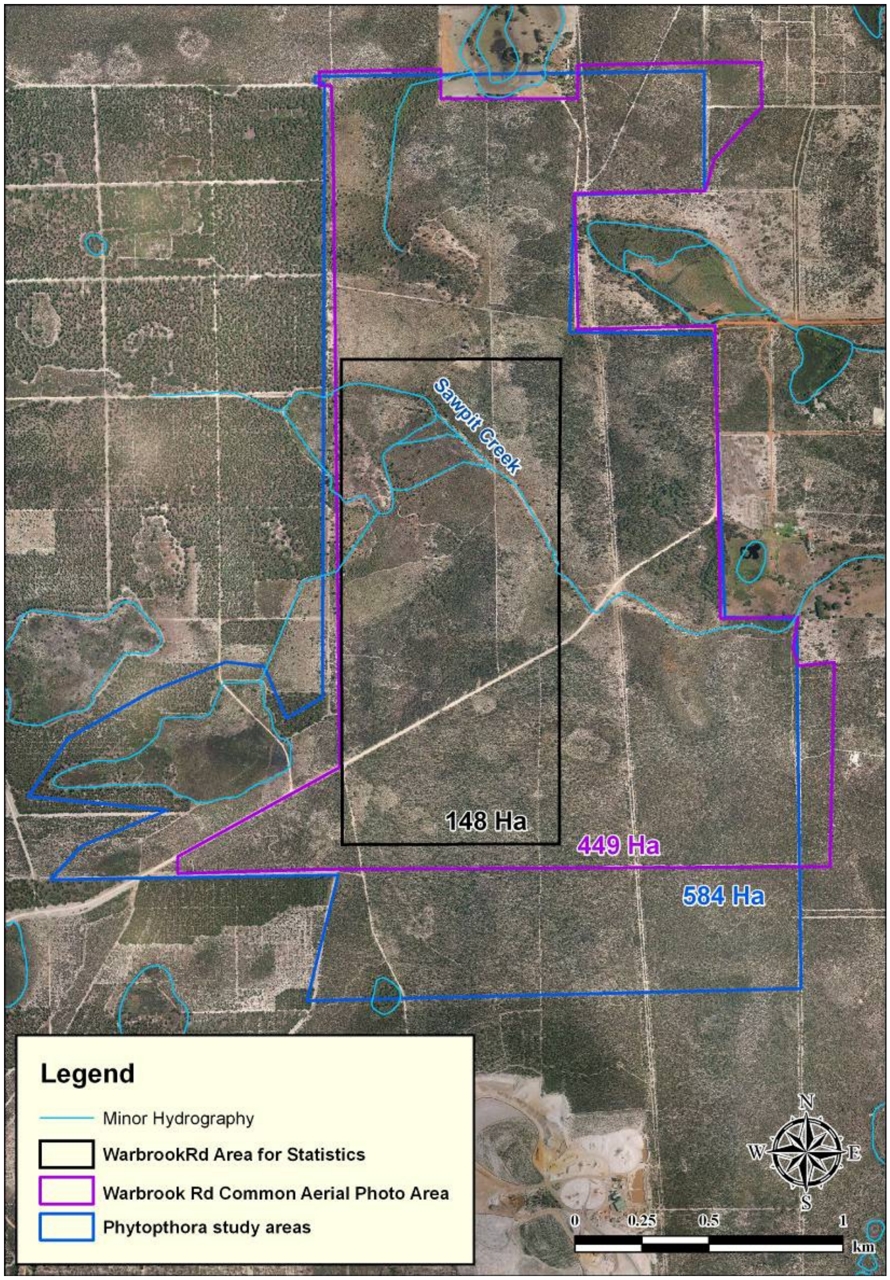

Figure 4: Warbrook Road study area boundaries used in analysis displayed on 2008 orthophoto: black area delineates area of good quality mapping used in the lineal measurement statistical analysis; the purple area delineates the common area in all orthophotos used for the across site areal assessment; and the blue area delineates the *Phytophthora* study area of Warbrook Road.

Rate of Spread

Determining front movement using GIS methods

In order to determine a rate of spread of the pathogen, linear measurements of the growth of disease impact areas is required. This was undertaken by using digitised disease impact areas which were extracted for each orthophoto date for a small area (hereafter referred to as the "Warbrook road area for statistics") of the common orthophoto area. The "Warbrook road area for statistics" is indicated by a black line on Figure 4. This area was chosen as the map quality was high for all years of orthophotos and thus the digitised fronts illustrate a continuous measurement of disease impact spread. Lineal measurements were taken by utilising two adjacent years to create an epoch in which perpendicular lines one metre apart were generated from the earliest year in the epoch and terminating at the second year in the epoch. This was undertaken using ET Geo Wizards 9.8 (Tchoukanski 2008) Create Station Lines tool, within ArcGIS 9.1. Figure 5 illustrates the construction of the measurement lines of disease impact spread. Any overlapping measurement lines were removed as the rate can not be clearly determined. Also a limit of 40 m was applied to the length, as larger impact movements are likely to be due to a combination of factors rather than the unassisted movement of the pathogen through the landscape, for example grazing.

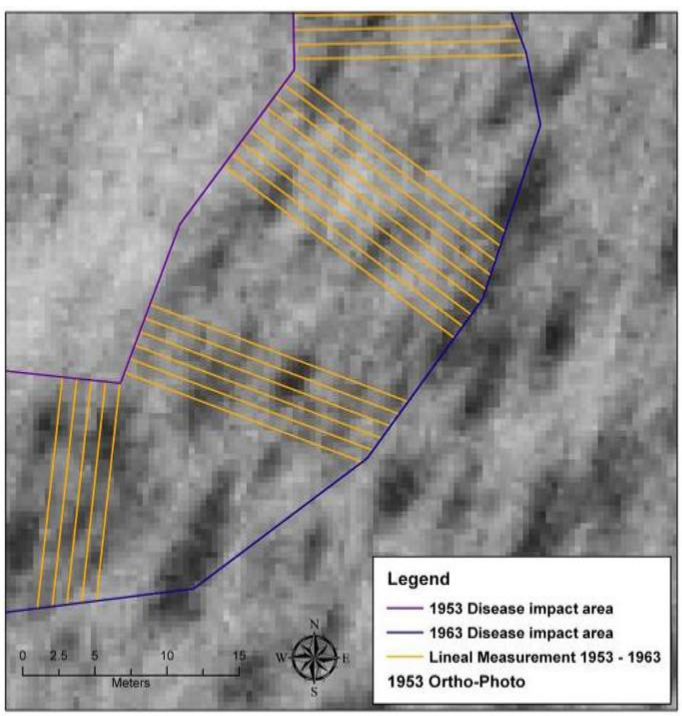

Figure 5: Lineal measurement of disease impact area spread.

Calculation of Linear Rate of Spread

The rate of spread of the disease impact was calculated per epoch as meters per year. The dataset used to calculate rate of spread was a subset of length measurements between digitised fronts in the "Warbrook road area for statistics" where disease impact mapping is of a high quality (Figure 4). A stratified random selection of lengths from each orthophoto epoch was used to determine the average rate of spread for each orthophoto epoch.

Examination of the interaction of the landscape attributes and the rate of spread can provide insights into the conditions that affect the speed of the spread of the pathogen. Movement of the disease can also be dependent on the availability of non-diseased areas with particular landscape characteristics. The dataset was thus stratified by orthophoto epoch, vegetation code and slope directions to ensure enough randomly selected features are present in each landscape variable category for statistical analysis. A total of 200 lengths were randomly selected in each stratum.

The spatial resolution of the landscape variables based on raster data is 10 m, and from the rate of spread results for each epoch it takes on average at least 10 years for the disease front to spread this distance. Therefore to accommodate this issue the impact between 1988-1997 and 1997-2008 was examined. New length segments were generated between each of these dates and attributed with the landscape variables. The stratified random sampling was applied to these new 10 year epochs and rate of spread calculated. For consistency the approximate 10 year epochs will be used when examining the landscape and climate variables.

Extracting landscape attributes using GIS methods

GIS methods were used to extract landscape attributes along the linear measurements of disease movement and infected and unaffected areas of the landscape.

The creation of the linear measurements between each epoch provides an observation set of disease impact in the landscape. As the observation sets are spatially referenced lines, other information on landscape variables from other spatial datasets can be extracted and attributed onto the length measurement lines. The datasets used to attribute the lines are listed in Table 4, and Figure 2 illustrates their values across the Warbrook Road site. When attributing each line across raster datasets the weighted linear mean was used, this takes into account the line crossing several raster cells and weights the value of the cells intercepted by more of the line to calculate the attribute. The raster cell values at the beginning of the line (earliest year in epoch) and at the end of the line (latest year in epoch) were also attributed to the line. The attribution of the lines with the vector datasets utilised a spatial join which joins the attributes of the first polygon encountered. This process produces an observation set for each epoch that is attributed with the following landscape variables:

- epoch,
- length,
- vegetation code,
- soil map unit,
- mean elevation,
- elevation at start of line,
- elevation at end of line,
- aspect,
- mean depth to water (2005),
- depth to water (2005) at start of line,
- depth to water (2005) at end of line,
- year of original infection and
- map quality.

Infected and uninfected areas

Polygons representing the area of disease impact between two dates were created using the digitised fronts. This was done to examine the landscape characteristics of infected and uninfected areas for each epoch. If the movement of the disease is found to be influenced by landscape factors, the availability of uninfested areas with these particular landscape characteristics will also influence the rate of spread of the disease in subsequent epochs. An approach using a grid of points was employed, as shown in Figure 6, to provide a sample observation set of disease status and landscape factor categories across the 'Warbrock Area for statistics" area. The grid points are 10 m apart to accommodate the resolution of the raster data and are attributed with the following landscape variables:

- epoch,
- vegetation code,
- soil map unit,
- elevation,
- aspect,
- depth to water (2005)
- year of original infection and
- map quality.

The amount and proportion of infected and uninfected area in each landscape category was calculated for each available orthophoto epoch.

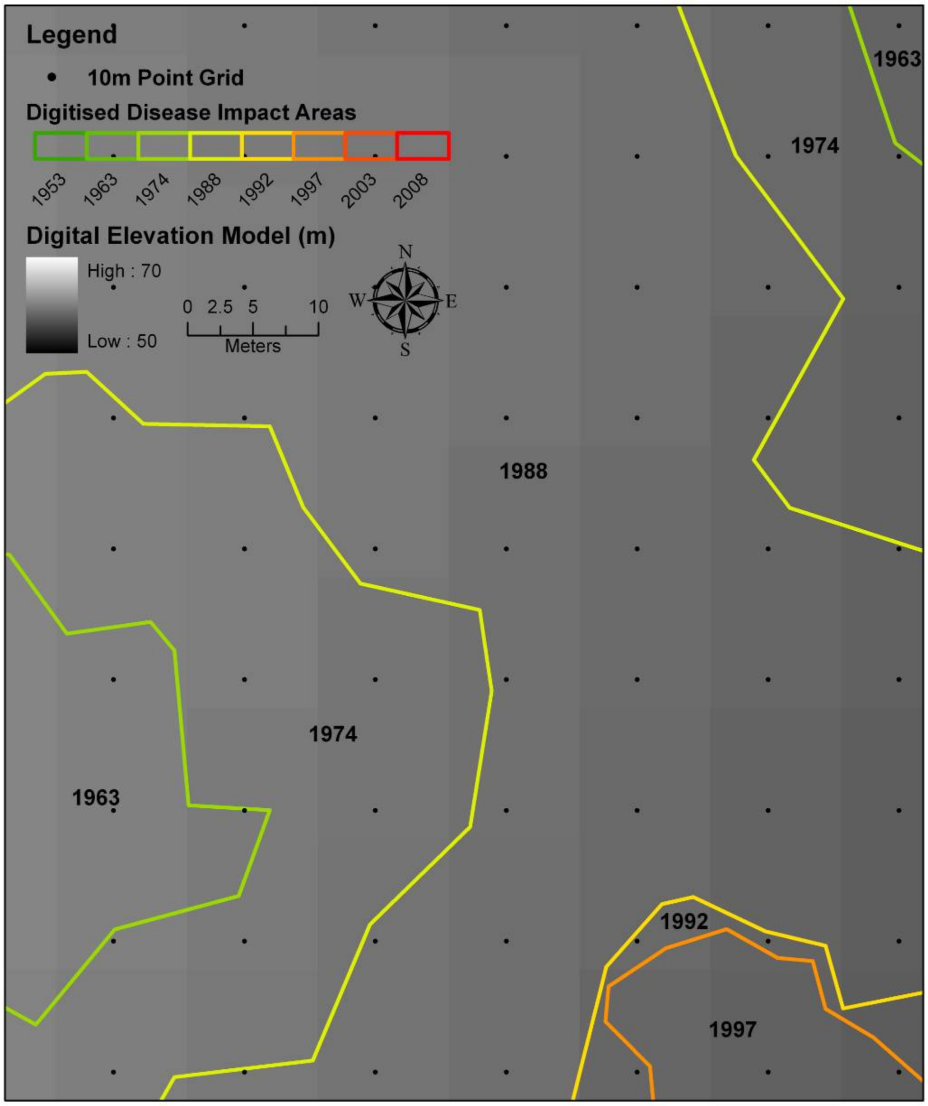

Figure 6: Attribution of 10 m grid points with epoch and elevation.

Statistical Analysis

Statistical analysis of the attributed spatial datasets created in the GIS provides insights into the interaction of landscape variables in the progression of *Phytophthora* through the study area. The main variable of interest was the rate of spread of *Phytophthora cinnamomi*. This variable was calculated using the linear measurement between epochs that represents the spread of *Phytophthora*. Linear lengths were standardised by epoch length (years), providing a measurement of the rate of spread of *Phytophthora* in metres per year. This standardises the length measure for each epoch and allows comparisons between epochs. The rate of spread was also examined in relation to a number of other landscape factors (Table 4), with categories within each factor. Continuous data, such as elevation, depth to water [2005] and aspect, were grouped into categories based on the distribution of the attributes in the infected areas and the whole study area. Additional factors were derived from these landscape attributes, including change and direction of elevation, and change and direction of depth to water, to examine the effect of slope magnitude and direction on pathogen movement. The set of lineal measurements derived from the approximate ten year epochs was used for analysis.

To explore patterns in data, one-way ANOVAs (using SPSS 2008, version 17.0) were used to examine differences in the rate of spread among a number of factors (epoch, vegetation code, soil map unit, elevation category, elevation change, depth to water [2005] category, depth to water [2005] change). Post-hoc Tukey HSD tests were used to determine differences among categories within a factor where applicable. We used the single-factor ANOVAs as a technique of identifying factors that may be influencing the rate of spread. We were specifically interested in examining the main drivers accelerating pathogen spread. To further explore these factors we examined a number of multi-factor ANOVAs, specifically to detect interactions among factors. As a number of factors were similar in the attribute they represented (e.g. elevation category and elevation change), we selected the factor we thought better described the relationship of rate of spread. Multi-factor ANOVAs were conducted on the following combinations of variables: a) epoch, vegetation code, depth to water [2005] category; b) epoch, vegetation code, elevation change; and c) epoch, vegetation code and slope direction.

Table 5: Linear disease movement measurements landscape categories for statistical analysis.

Factor	Categories	Definition
Epoch – beginning and end year which front movement is measured between	1953_1963	9.3yrs – 15/12/1953 to 3/04/1963
	1963_1974	9.8yrs – 3/04/1963 to 10/07/1974
	1974_1988	12.8yrs – 10/07/1974 to 5/04/1987
	1988_1992	5.8yrs – 5/04/1987 to 15/12/1992
	1988_1997(created to provide ~10yr epoch)	9.8yrs – 5/04/1987 to 5/01/1997
	1992_1997	4yrs – 15/12/1992 to 5/01/1997
	1997_2003	6yrs – 5/01/1997 to 01/2003
	1997_2008 (created to provide ~10yr epoch)	11yrs – 5/01/1997 to 01/2008
	2003_2008	5yrs – 01/2003 to 01/2008
Rate per Year – rate of disease impact growth in meters per year	Real numbers (m/yr)	Length measured between epoch fronts divided by number of years
Vegetation Code – code of vegetation type from Mattiske 2003 vegetation mapping	I1	Low Open Woodland of *Banksia attenuata*
	J1	Woodland of *Corymbia calophylla, Banksia attenuatae, Banksia menziesii, Melaleuca preissiana*
Soil Map Unit – soil mapping from the Dept. of Agriculture and Food Western Australia	212Bs__J	Poorly drained depressions
	212Bs__Ja	Jandakot low dunes. Slopes < 10% and generally more than 5m relief
	213Ya_8x	Flat plain with occasional low dunes. Subject to seasonal flooding.
Slope Direction – created from 15m segments orthogonal to first year front and subtracting beginning and end DEM values i.e. DEM start – DEM end(15m)	Flat	Change in height between -0.09m and 0.09m
	Uphill	Negative change in height
	Downhill	Positive change in height
DEM Category – average elevation value across length categorized into descriptive classes, gives insight into position in landscape	Low	55-60m (AHD)
	Low mid	60-65m (AHD)
	Mid	65-70m (AHD)
	High	70-75m (AHD)
DEM Change Category – height at first year of line segment subtract the height at end of line segment at second year of epoch categorized into descriptive classes	Steep uphill	DEM Change -0.5 to -2.0m
	Uphill	DEM Change -0.2 to -0.5m
	Slight uphill	DEM Change -0.09 to -0.2m
	Flat	DEM Change -0.09 to 0.09m
	Slight downhill	DEM Change 0.09 to 0.2m
	Downhill	DEM Change 0.2 to 0.5m
	Steep downhill	DEM Change 0.5 to 2.0m
Aspect Category – average aspect across the length in degrees derived from 10m DEM divided into 4 major and 4 minor directions	North	0º-30º and 330º-360º
	North East	30º-60º
	East	60º-120º
	South East	120º-150º
	South	150º-210º
	South West	210º-240º
	West	240º-300º
	North West	300º-330º
DTW (2005) Category – average depth to water (2005) across the length categorized into descriptive classes	Surface	-10 to 0m
	Near surface	0 to 5m
	Shallow	5 to 10m
	Mid shallow	10 to 15m
	Mid deep	15 to 20m
	Deep	20 to 25m
	Very deep	25 to 30m

Factor	Categories	Definition
DTW (2005) Change Category – DTW at first year of line segment subtract the DTW at end of line segment at second year of epoch categorized into descriptive classes	Steep upgrade	DTW Change -0.5 to -3.0m
	Upgrade	DTW Change -0.2 to -0.5m
	Slight upgrade	DTW Change -0.09 to -0.2m
	Flat	DTW Change -0.09 to 0.09m
	Slight downgrade	DTW Change 0.09 to 0.2m
	Downgrade	DTW Change 0.2 to 0.5m
	Steep downgrade	DTW Change 0.5 to 3.0m
Original Infection Date – year PC front is first detected, indication of virulence	Integer	1953, 1963, 1974, 1988, 1992, 1997, 2003

Climatic Factors

The data available for climate variables such as rainfall and temperature do not have the spatial resolution of the landscape variables. These climate data do have high temporal resolution; and so can be compared with measurements from each epoch. Climate variables derived for analysis include; average monthly rainfall per epoch, average maximum temperature per epoch and average minimum temperature per epoch.

Results

Using Remote Sensing Tools to identify impact areas

Trends in vegetation cover derived from Landsat imagery were useful in aiding the identification of *P. cinnamomi* affected areas. The linear trends provided information on those areas of the landscape where cover had declined during the last 20 years. Some areas that had been infected for a number of years did, however, exhibit fluctuating trends, indicating vegetation cover had increased sometime during the period, possibly from colonisation by resistant species or post infection invasive colonising taxa (e.g. weeds) (Figure 7). The low resolution of Landsat data (25 m) means that Landsat trends alone cannot be used to map the extent of disease affected areas. Rather, when historical aerial photos are not available, Landsat trends can provide useful data on vegetation cover over time to help determine if changes in vegetation cover are likely to be associated with *P. cinnamomi* impacts or other processes such as fire, clearing or grazing.

An example using aerial photography and Landsat trend analysis (1988–2007) of the extent of the *P. cinnamomi* infestation is shown in Figure 7.

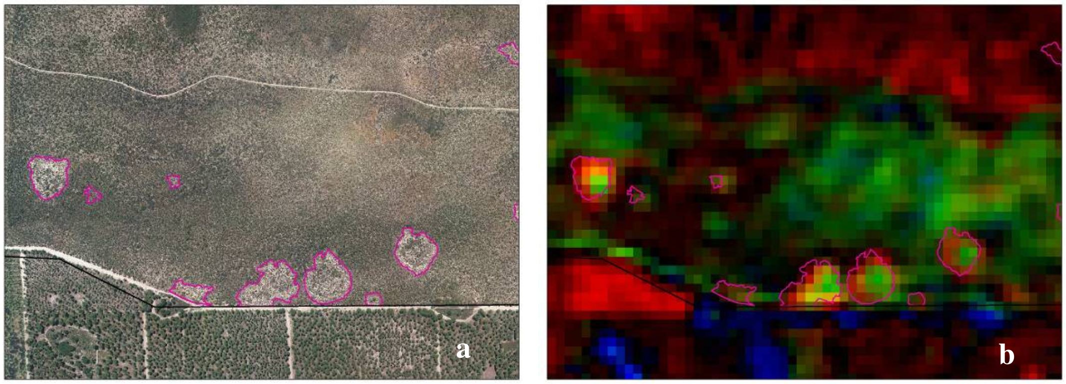

Figure 7: (a) 2008 Aerial photograph north of Gnangara Pine Plantation showing extent of the disease (pink lines) in 2008 and (b) the Landsat vegetation trends (1988-2007) for the area. (Trends- red - major negative, orange–yellow -negative, green- fluctuating, blue - positive, black- no change).

A combination of interpretation of orthophotos and Landsat Trend information was successful in identifying *P. cinnamomi*- impacted areas in the Warbrook Road, Pinjar and Gnangara study areas (Figure 8 and Figure 9). No *P. cinnamomi*-impacted areas were identified in the Neaves study area and this was consistent with the results of the ground-based surveys. Comparison of the mapped boundaries for the Warbrook Road and Gnangara study areas with the ground based survey mapping revealed that the majority of infected areas had been identified though the boundaries were not always aligned (Figure 9). This may reflect that the ground-based methods are better able to discriminate diseased areas based on deaths of individual understorey species even when susceptible overstorey species have not yet declined. In comparison orthophoto interpretation relies more on the death of overstorey susceptible species and subsequent loss of cover. Field validation of the Pinjar site was more limited but of the 12 mapped areas visited all but one were determined to be infected with the disease.

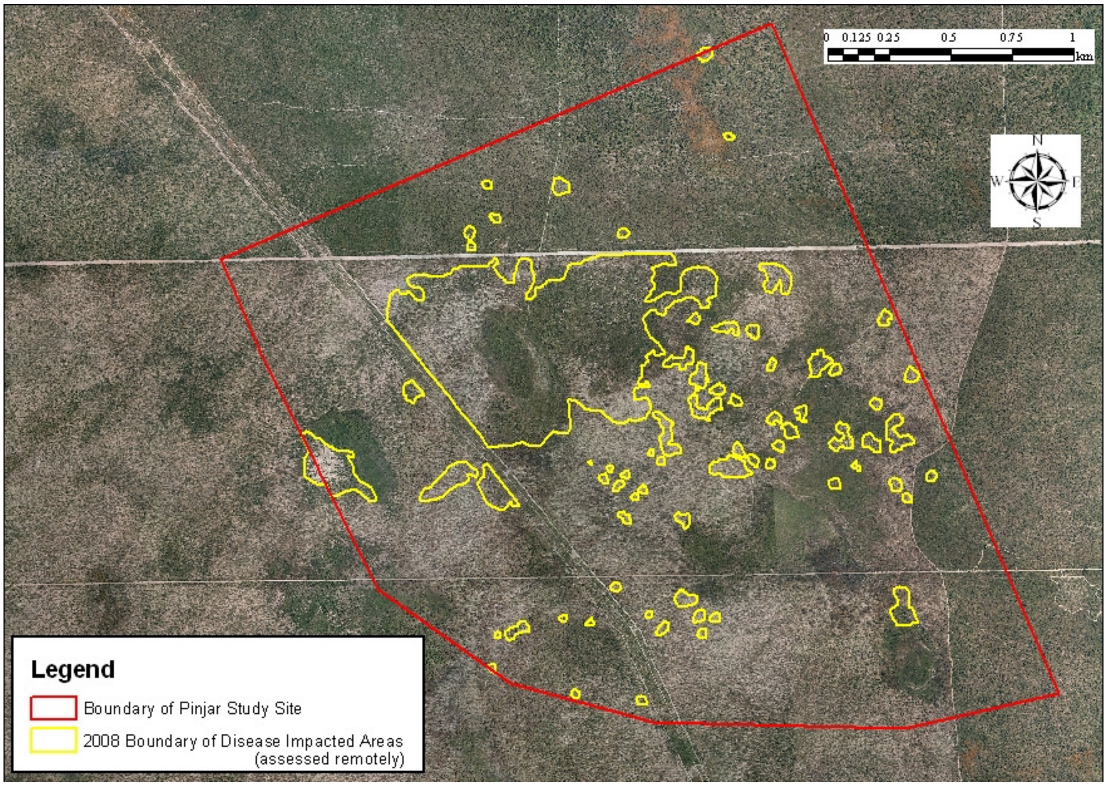

Figure 8: The extent of areas assessed to be impacted by *P. cinnamomi* using orthophoto interpretation methods and information from Landsat Trend analyses for the Pinjar study area.

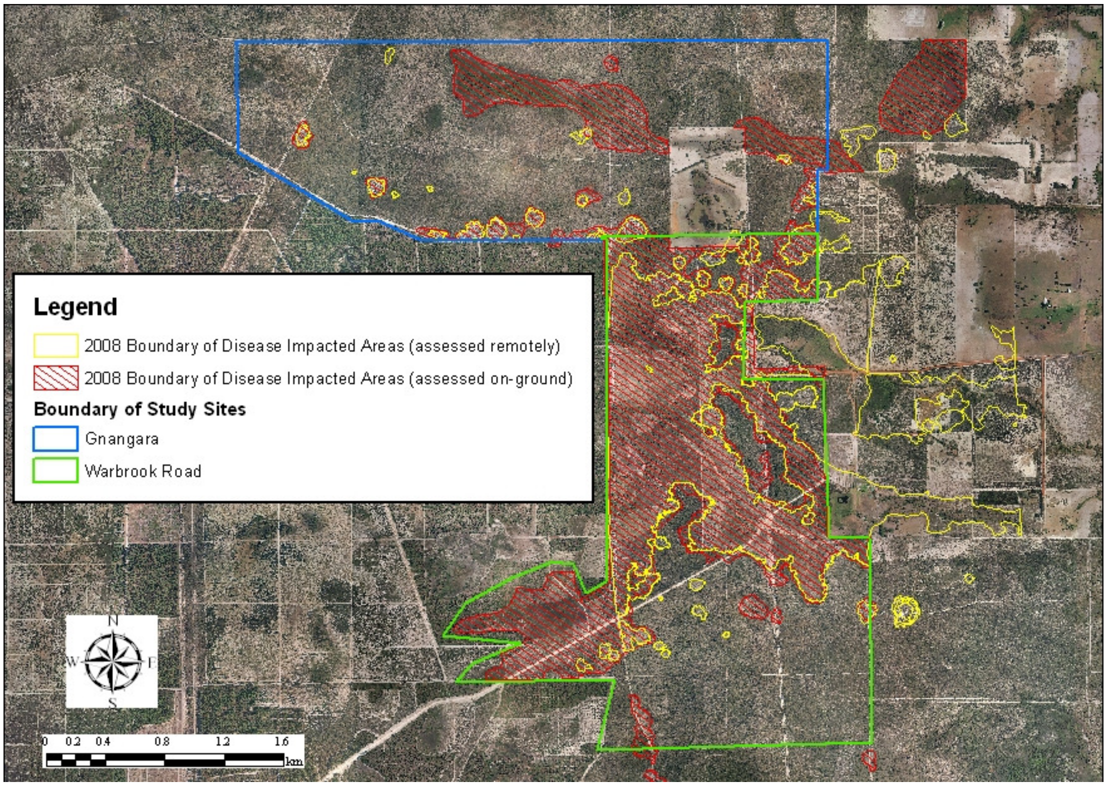

Figure 9: The extent of areas assessed to be impacted by *P. cinnamomi* using orthophoto interpretation methods and information from Landsat Trend analyses for the Gnangara and Warbrook Road study areas. Also shown on the map are the boundaries of disease areas as assessed by ground-based methods for the Warbrook Road and Gnangara study areas.

Current and historical extent of impacted areas at Warbrook Road

A substantial proportion of the Warbrook Road area was impacted by *Phytophthora* dieback prior to 1953 (Table 6; Figure 10 and Figure 11). Hill *et al.* (1994) determined that the initial infection of the Warbrook Road area is likely to have occurred before 1942 and that during subsequent decades the swamp complex at the site became contaminated, initiating disease fronts several kilometres long. Our analysis found that there was a large increase in impacted areas between 1974 and 1988 reflecting the length of the time between dates and the identification of several new infections in 1988. Further in 1988 there were several discrete disease fronts which have in subsequent years coalesced to form two long fronts in the south-west and north-east of the study area (Figure 10). The area of infestation by the pathogen increased substantially over the 55 years starts from 14% of the area to 47%.

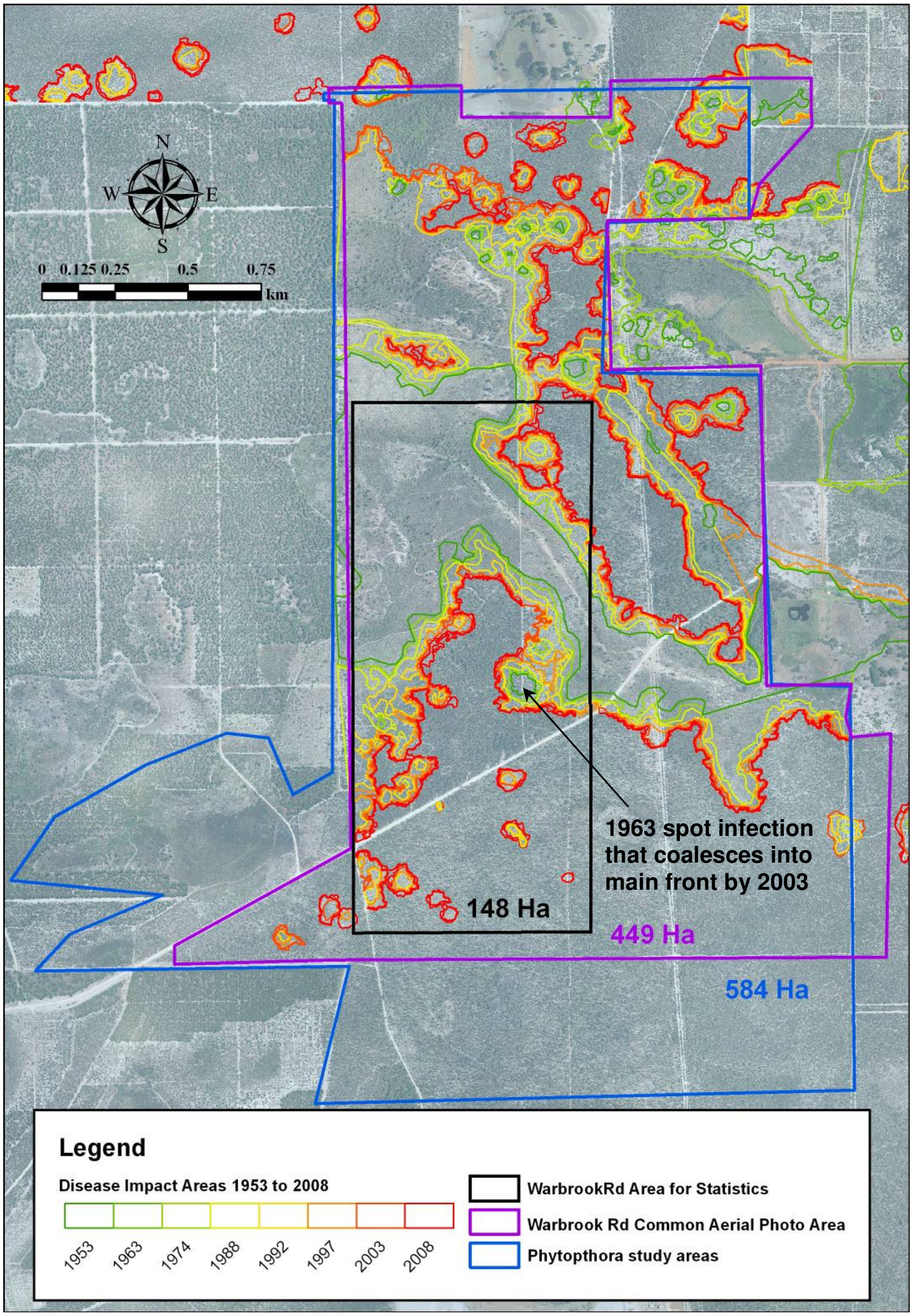

Figure 10: Digitised disease impact areas and study areas used in analysis displayed on 2008 orthophoto, black area delineates area of good quality mapping used in the lineal measurement statistical analysis and the purple area delineates the common area in all orthophotos used for the across site areal assessment and the blue area delineates the *Phytophthora* study area of Warbrook Road.

Table 6. Total cumulative area and the proportion of the Warbrook Road common orthophoto study area, infected with *P. cinnamomi* for a number of years.

Orthophoto Year	Cumalative Area (Ha)	Proportion of study area infected (%)
1953	64.897	14.445
1963	74.664	16.619
1974	101.125	22.509
1988	160.186	35.656
1992	179.530	39.962
1997	195.059	43.418
2003	205.999	45.853
2008	214.171	47.673

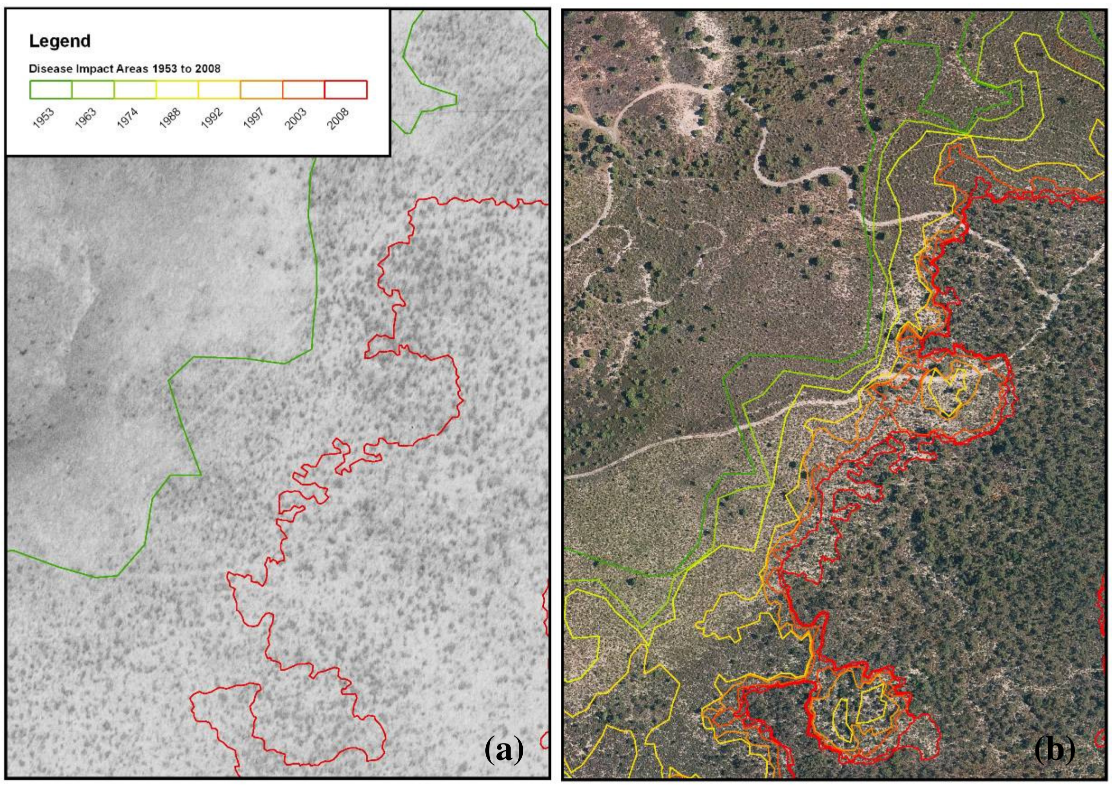

Figure 11: Detail of aerial photographs of the study area in (a) 1953 and (b) in 2008. In (a) the lines show the extent of the disease in 1953 and 2008 and in (b) all time periods. Note the coalescence of discrete patches to form continuous fronts.

Landscape factors in disease impacted areas

To assess the availability of uninfected areas in relationship to different landscape categories the proportion of infected and uninfected area of each landscape category was determined for each epoch. The attributed 10 m grid points were used to determine the percentage of each category impacted per epoch. Initially 50% of the I1 (Low open *B. attenuata* woodland) vegetation type was infected and only 10% of J1 (*Banksia, Melaleuca* woodland). Post 1997 the % of J1 infected increased to 20-30% and I1 to 80-90% (Figure 12a). In 1953 three soil types had 50-80% infested (212Bs__G (flat undulating, humus podzols), 212Bs__J (poorly drained depressions, humus podols) and 213 Ya-8x) (flat plain subject to floods, white-yellow sands, some swamp) and all increased to 60-100% post 1974. As the availability of uninfected areas post 1974 in the soil types declined, or became totally infested, the proportion of area infested for soil type 212Bs_Ja (Jandakot low dune, grey sand) increased from 10% pre 1974 to 20-30% post 1974 (Figure 12b). Over the time period deeper depths to ground water became infected (Figure 12c) and the impacted areas increased from the lower to higher parts of the landscape (Figure 12d). Areas of infection for all aspects increased post 1974, and particularly for the north west aspect (Figure 12e).

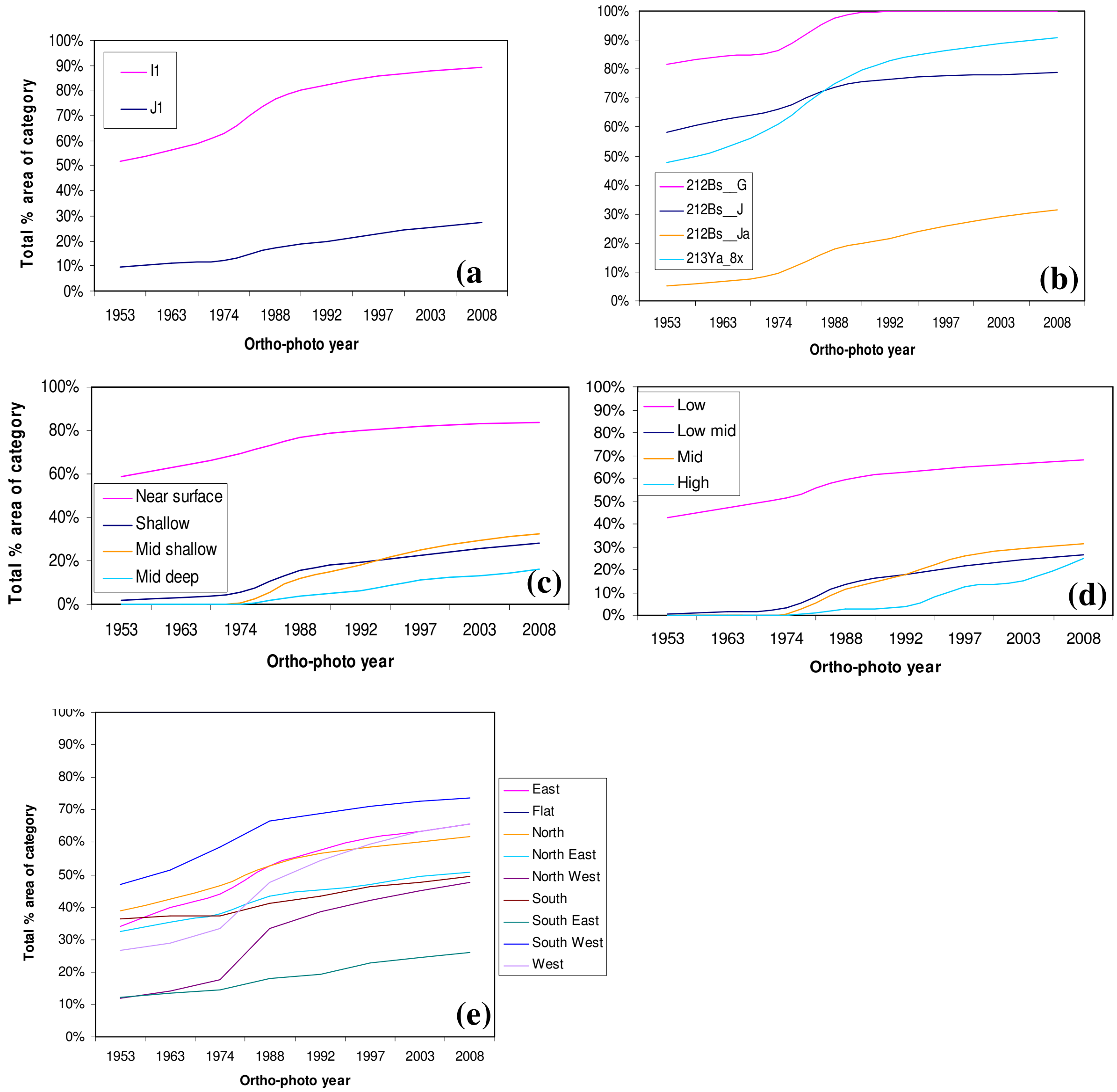

Figure 12: Graphs of cumulative disease impact as a percentage of total area occupied by each landscape category; a) vegetation code, b) soil map unit, c) depth to water 2005 category, d) DEM category (AHD) and e) aspect.

Linear Rate of Spread

The average rate of spread for each epoch between all orthophoto dates using the random selection is shown in Figure 13, figures and numbers of observations are available in Appendix C. The rate of spread declined from 1.286 m/yr in 1953-63 to 0.526 m/yr in 1997-2008. Thus in more recent years the rate of spread decreased considerably and the possible factors contributing to the decline such as landscape features and a drying climate are examined in the following sections.

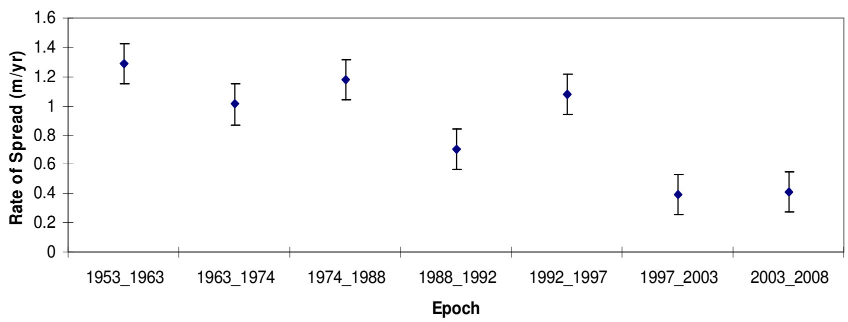

Figure 13: Rate of spread (m/yr) of pathogen impact between every available orthophoto date with standard error bars.

The average rate of spread for the approximate 10 year epochs is illustrated in Figure 14. The rate of spread among epochs varied significantly (ANOVA: $F_{4,4652} = 219.351$, $P< 0.001$). All 10 year epochs had significantly different rate of spread from one another (Tukey HSD, $P< 0.01$) except for 1963-1974 versus 1988-1997.

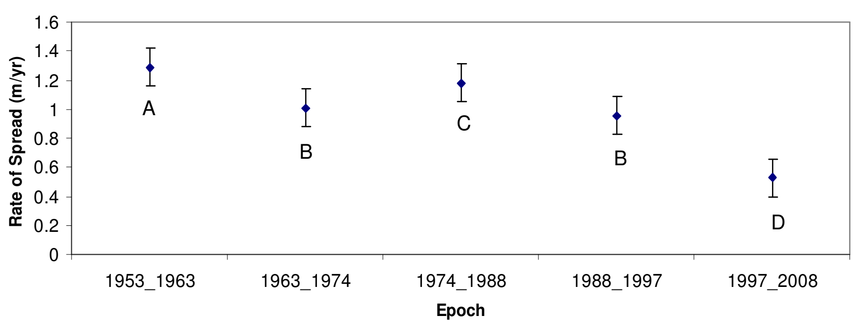

Figure 14: Rate of spread (m/yr) of pathogen impact between orthophoto dates approximately 10 years apart with standard error bars. Letters below error bars indicate significant differences of means between epochs (Tukey HSD, $P< 0.01$).

Landscape factors

Single-factor ANOVAs were used to identify factors that may be the main ones accelerating pathogen spread and then we examined a number of multi-factor ANOVAs, specifically to detect interactions among factors.

Single Factor ANOVA

The average rate of spread of disease front movement in the 10 year epochs was assessed for relationships with which landscape attributes may affect pathogen spread (Table 7; Figure 15 to Figure 22). The rate of spread varied between all the factors examined, including epoch, vegetation code, soil map unit, elevation change (DEM Change), landscape elevation (DEM Category), landscape depth to water (DTW(2005) Category) and depth to water change (DTW (2005) Change).

There was a significant difference in the rate of spread of the pathogen between all three soil map units (Figure 15). The rate of spread was greatest in humus podzols of the poorly drained depressions (soil map unit 212Bs__J) and higher on soil map unit 213Ya_8x (Yanga soils of white sands interspersed with swamps) compared to 212Bs_Ja (grey sands). Landscape elevation affected the rate of spread (Table 7; Figure 16), with low and low mid landscape elevations exhibiting a faster rate of spread. Differences in the changes in elevation (DEM Change) significantly influenced the rate of spread (Table 7; Figure 17), with flat areas having a slower rate of spread and the rate increasing with steepness of change regardless of direction. DEM Change categories are for the most part, different to one another, (Tukey HSD, $P<0.01$), and displayed a consistent relationship between steepness and rate of spread. The landscape depth to water categories indicated that the closer to the surface the groundwater was, the faster the rate of spread (Table 7; Figure 18). The rate of spread was reduced in the mid-shallow and mid-deep categories, indicating that there is a depth to water threshold whereby the rate of spread is reduced. We detected a significant difference in the rate of spread among depth to water change categories (Table 7; Figure 19), however, these differences were only between flat and any grade change (i.e. upgrade or downgrade).

Disease impact spread was at a higher rate in J1 compared to I1 vegetation type (Table 7; Figure 20; Appendix A). The average rate of spread in the aspect categories is fastest in the southerly direction (Table 7; Figure 21) and there are mostly no significant differences between the other aspect categories. The slope direction categories showed that the rate of spread was greater uphill than on the flat and downhill slopes (Table 7; Figure 22).

Table 7: ANOVA F-values for epoch, vegetation code, soil map unit, DEM change, DEM category, depth to water (2005) category, depth to water (2005) change, aspect and slope direction.

Factor (df)	**F**
Epoch (4,4652)	219.351***
Vegetation Code (1, 4655)	5.573*
Soil Map Unit (2, 4654)	74.306***
DEM Change (6, 4650)	226.763***
DEM Category (3, 4653)	134.322***
DTW (2005) Category (3,4653)	141.140***
DTW (2005) Change (6,4650)	236.080***
Aspect (7,4649)	6.324***
Slope Direction (2,4654)	95.353***

* $P < 0.05$, ** $P < 0.01$, *** $P < 0.001$.

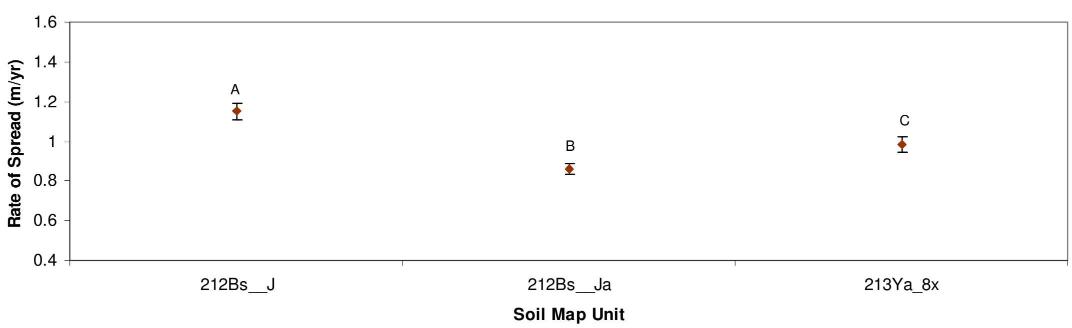

Figure 15: Rate of spread (m/yr) of pathogen impact in soil map units with standard error bars. Letters below error bars indicate significant differences of means between epochs (Tukey HSD, $P < 0.001$).

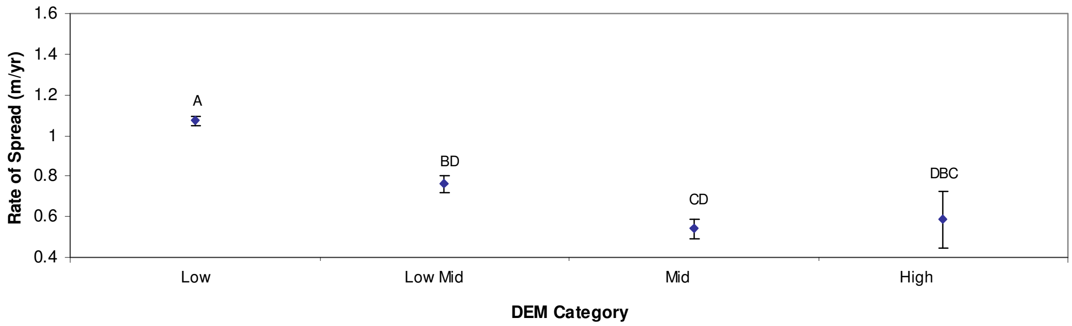

Figure 16: Rate of spread (m/yr) of pathogen impact in DEM categories with standard error bars. Letters below error bars indicate significant differences of means between epochs (Tukey HSD, $P < 0.001$).

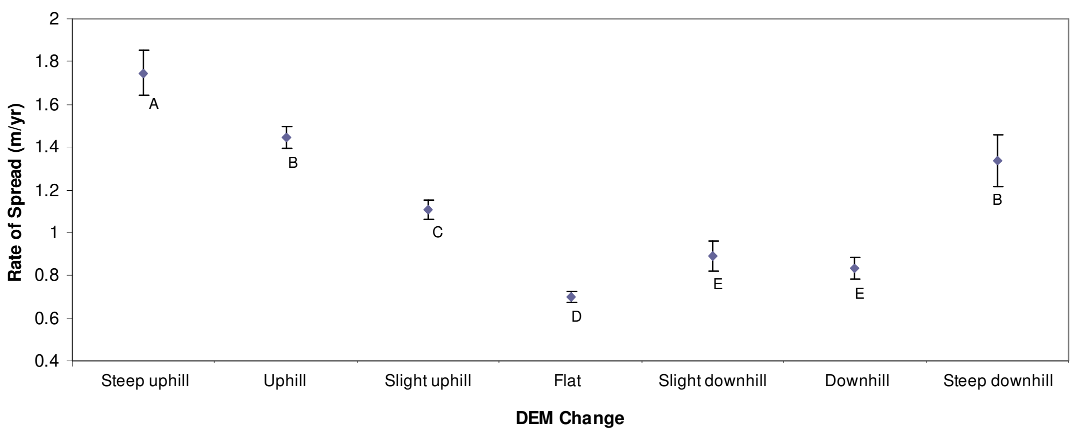

Figure 17: Rate of spread (m/yr) of pathogen impact in DEM change categories with standard error bars. Letters below error bars indicate significant differences of means between epochs (Tukey HSD, $P < 0.01$).

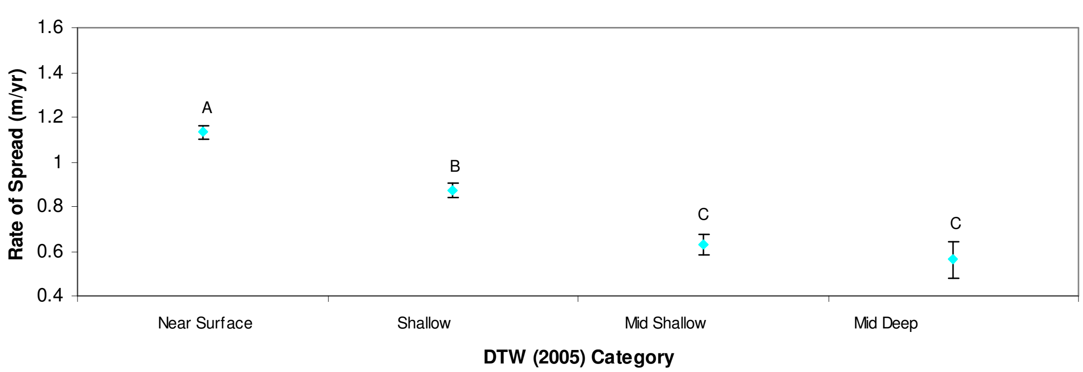

Figure 18: Rate of spread (m/yr) of pathogen impact in DTW (2005) categories with standard error bars. Letters below error bars indicate significant differences of means between epochs (Tukey HSD, *P*< 0.001).

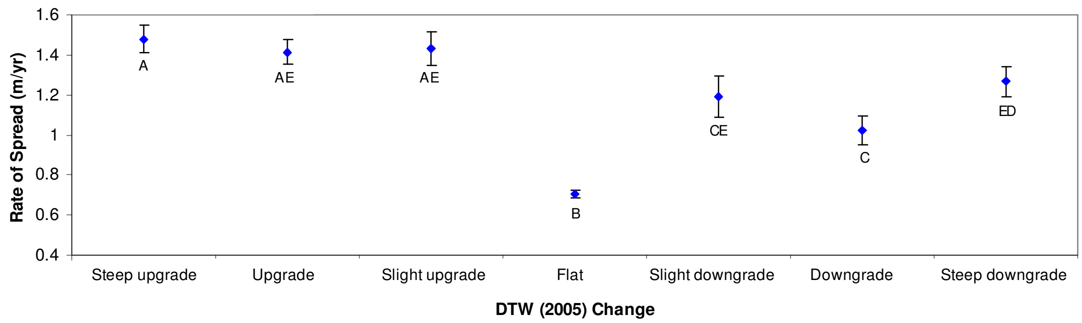

Figure 19: Rate of spread (m/yr) of pathogen impact in DTW (2005) change categories with standard error bars. Letters below error bars indicate significant differences of means between epochs (Tukey HSD, *P*< 0.001).

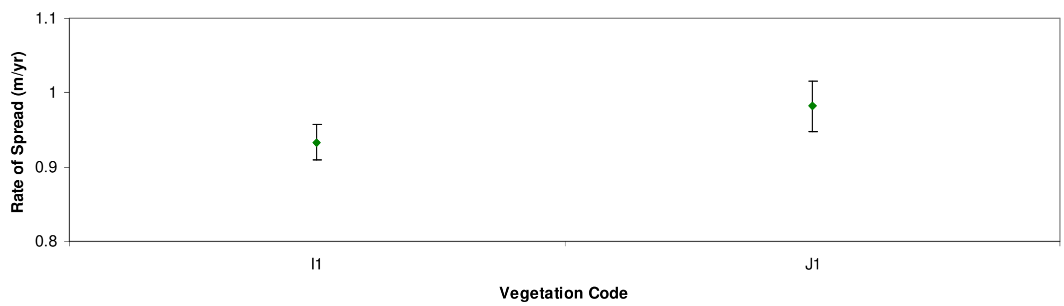

Figure 20: Rate of spread (m/yr) of pathogen impact in vegetation codes with standard error bars.

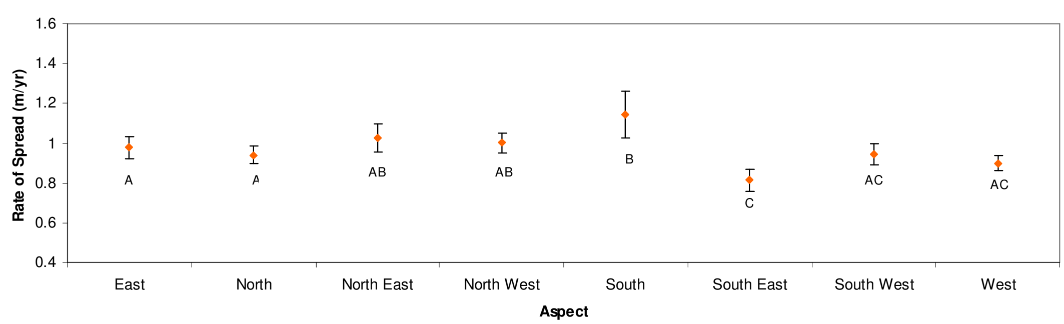

Figure 21: Rate of spread (m/yr) of pathogen impact in aspect directions with standard error bars. Letters below error bars indicate significant differences of means between epochs (Tukey HSD, *P*< 0.05).

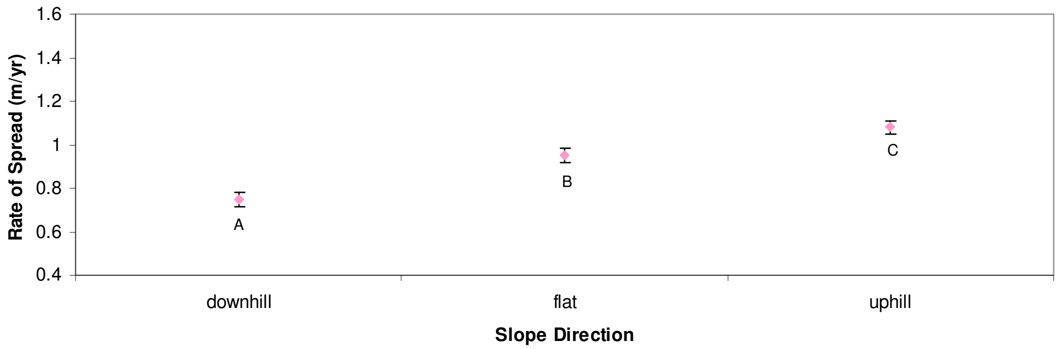

Figure 22: Rate of spread (m/yr) of pathogen impact on different slope directions with standard error bars. Letters below error bars indicate significant differences of means between epochs (Tukey HSD, $P < 0.001$).

Multiple Factor ANOVA

A significant interaction between epoch, vegetation type and depth to water ($P < 0.01$; Table 8) indicates that the rate of spread varies amongst different combinations of these factors. For vegetation type J1 the pathogen was restricted to areas with near surface depth to water in the 1953 – 1963 epoch and near surface and shallow areas in the 1963 – 1974 and 1974 – 1988 epochs and then was present in all depth to water categories in the two remaining epochs(Figure 23). Whereas for the I1 vegetation type, the pathogen was present over a wider range of depth to water categories in the first two epochs (Figure 23a and b) and then was present in all depth to water categories in the last three epochs (Figure 23c - 23e). Thus the pathogen is predominantly present only in the more shallow depth to water categories in the early years (Figure 12c).

There is a significant interaction between depth to water and epoch ($P<0.001$) indicating that rate of spread varies amongst different depth to water categories in different years (Table 8). The absence of the pathogen in the deeper depth to water categories in the early epochs prevents us from exploring this in detail.

No one vegetation type had a consistently faster rate of spread compared to the other within each epoch and depth to water categories (Figure 23). There were a few instances when vegetation type (J1) did have a faster rate of spread than vegetation type of I1. However, there was no clear trend with depth to water with these instances occurring over a range of depth to water categories (near surface 1953 – 1963, mid deep 1988 – 1997 and mid shallow 1997 – 2008; Figure 23a, c and d).

Table 8: Multiple ANOVA F-values of epoch, vegetation code and depth to water (2005) category. Dependent variable is rate of spread.

Source	**df**	**F**
Epoch	4	84.622***
Vegetation Code	1	15.829***
DTW(2005) Category	3	5.240**
Epoch * Vegetation Code	4	14.576***
Epoch * DTW(2005) Category	9	10.525***
Vegetation Code * DTW(2005) Category	3	2.812*
Epoch * Vegetation Code * DTW(2005) Category	5	3.541**
Error	4627	

* *P*< 0.05, ** *P*< 0.01, *** *P*< 0.001.

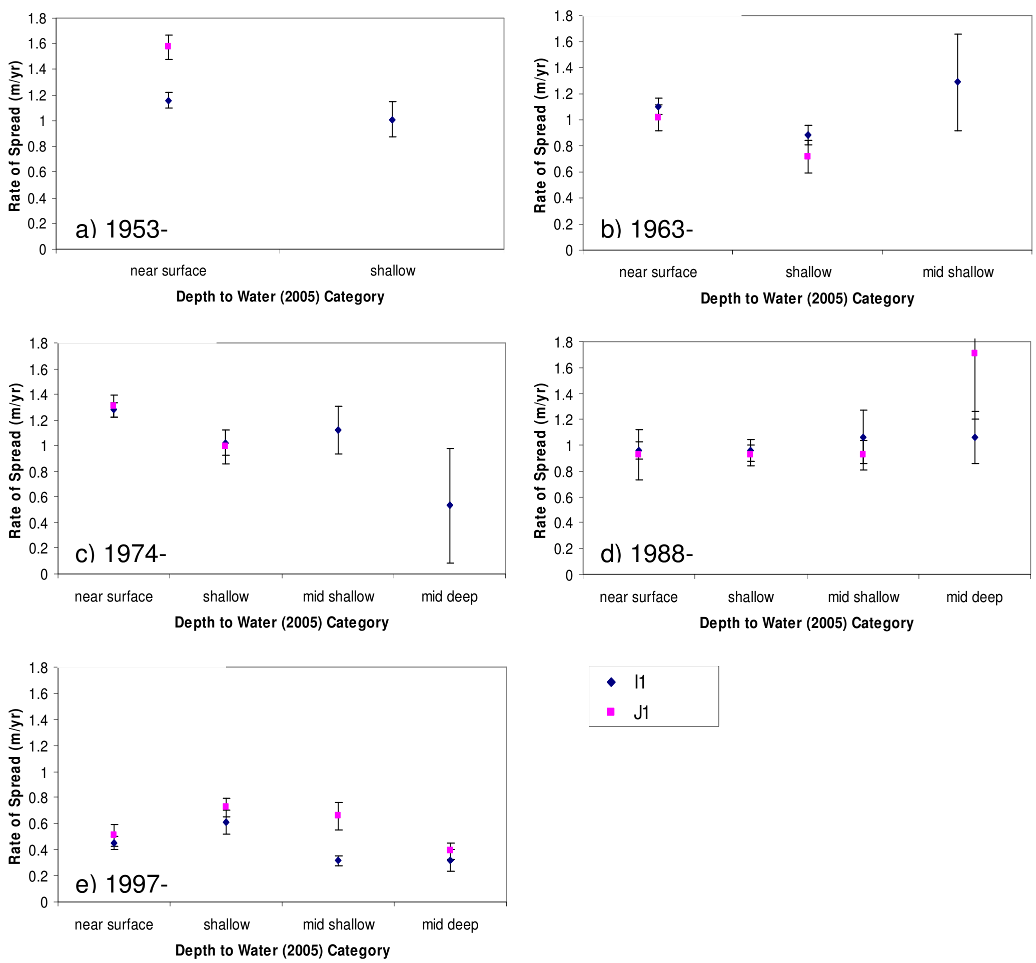

Figure 23: Average rate of spread (m/yr) grouped by depth to water (2005) category and vegetation type in each approximate ten year epoch a) to e).

A significant interaction between epoch, vegetation type and elevation change ($P < 0.001$; Table 9) indicates that the rate of spread varies amongst different combinations of these factors. In the first epoch (1953 – 1963) flat areas had the slowest rate of spread for both vegetation types (Figure 24a) and the pathogen was not yet present in the downhill areas of vegetation type J1. The fastest rate of spread in the 1953 – 1963 epoch occurred in steep uphill areas across both vegetation types and in the steep downhill areas of I1. This trend of slow rates of spread on flat areas and fast rates of spread on steep uphill or downhill areas continued for the next two epochs (1963 – 1974 and 1974 – 1988) for both vegetation types (Figure 24b and c). For the 1988 – 1997 epoch, the rate of spread is generally lower than the previous epoch's. For vegetation type I1, in the 1988 – 1997 epoch, the fastest rate of spread again occurred on steep uphill and downhill areas but the slowest rate of spread did not occur on downhill areas (Figure 24d). No trend with steepness and rate of spread was evident in vegetation type J1 for this epoch (Figure 24d). Across all elevation change categories and vegetation types in the final epoch (1997 – 2008) the rate of spread was a lot lower, in comparison to all other epochs, and no trend with steepness was evident (Figure 24e).

Table 9: Multiple ANOVA F-values of epoch, vegetation code and DEM Change. Dependent variable is rate of spread.

Source	**df**	**F**
Epoch	4	108.011*
Vegetation Code	1	.466
DEM Change	6	173.744*
Epoch * Vegetation Code	4	19.396*
Epoch * DEM Change	24	8.663*
Vegetation Code * DEM Change	6	8.470*
Epoch * Vegetation Code * DEM Change	21	5.424*
Error	4590	

* $P < 0.001$.

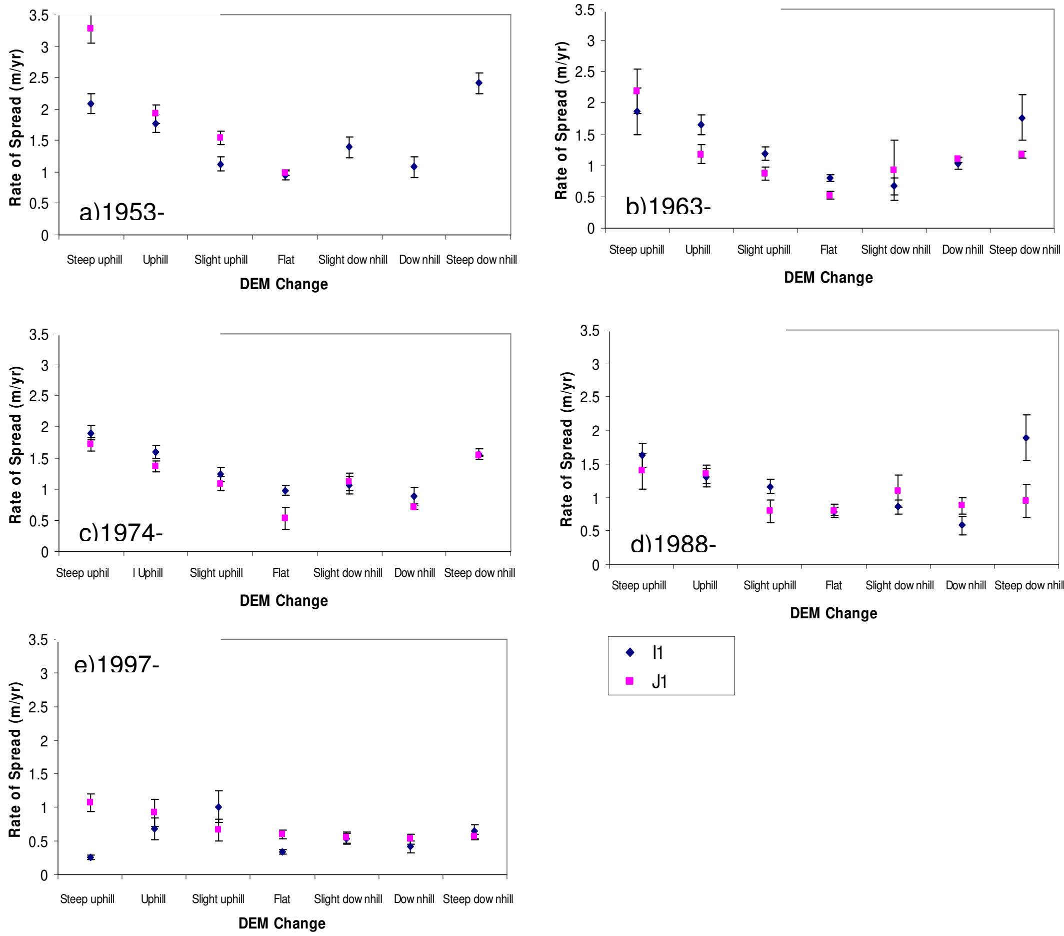

Figure 24: Average rate of spread (m/yr) grouped by DEM Change category and vegetation type in each approximate ten year epoch; a) to e).

A significant interaction between epoch, vegetation type and slope direction ($P< 0.001$; Table 10) indicates that the rate of spread varies amongst different combinations of these factors. In a similar pattern to depth to water and elevation change, rate of spread across all slope categories is a much lower in the final epoch (1997 – 2008).

There is no consistent trend between vegetation type and slope direction in the early epochs (1953 – 1963, 1963 – 1974 and 1974 – 1988; Figure 25a – c). In the epochs (1988 – 1992 and 1997 and 2008) the wetland vegetation type (J1) generally has a higher rate of spread across all slope directions (Figure 25d and e).

Table 10: Multiple ANOVA F-values of epoch, vegetation code and slope direction. Dependent variable is rate of spread.

Source	**df**	**F**
Epoch	4	156.553***
VegCode	1	2.751
SlopeDirection	2	35.499***
Epoch * VegCode	4	15.741***
Epoch * SlopeDirection	8	7.372***
VegCode * SlopeDirection	2	6.964**
Epoch * VegCode * SlopeDirection	7	20.220***
Error	4628	

* $P< 0.05$, ** $P< 0.01$, *** $P< 0.001$.

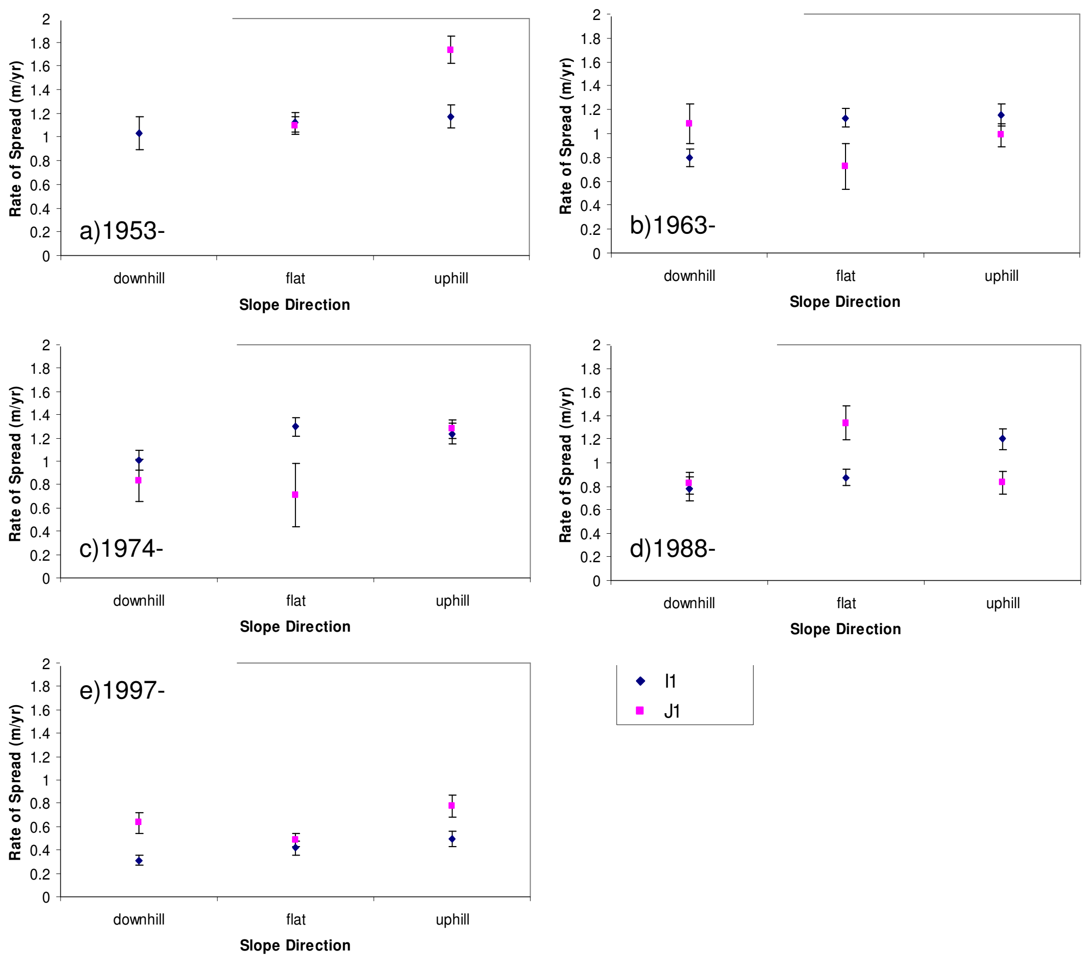

Figure 25: Average rate of spread (m/yr) grouped by slope direction and vegetation type in each approximate ten year epoch; a) to e).

Climate variables

The rainfall patterns in the study area have changed over the last 55 years. Rainfall patterns for the epochs 1953-1963 and 1963-1974 are very similar, but in the latter epochs there is a substantial drop in winter (June and July) rainfall with the last epoch 1997-2008 showing a much lower average than previous (Figure 26).

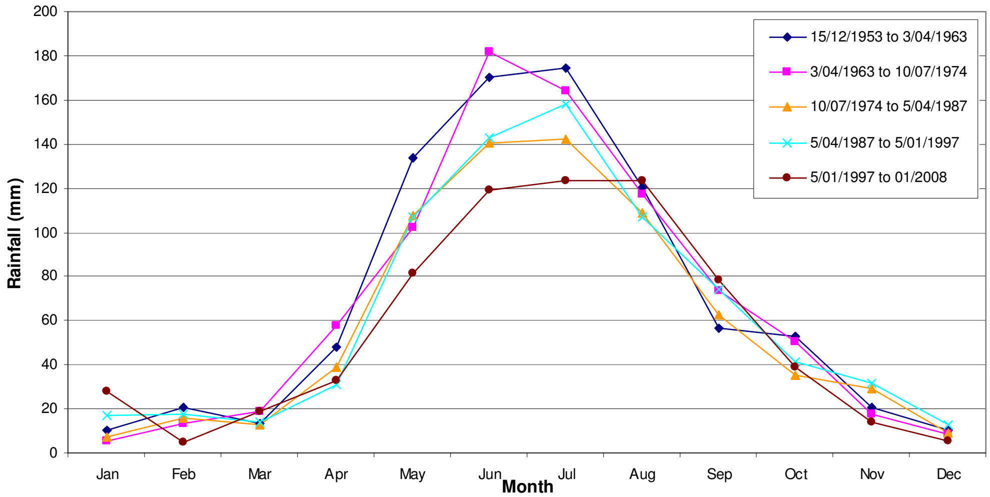

Figure 26: Average monthly rainfall per orthophoto epoch at station 9029 located at Muchea tree farm.

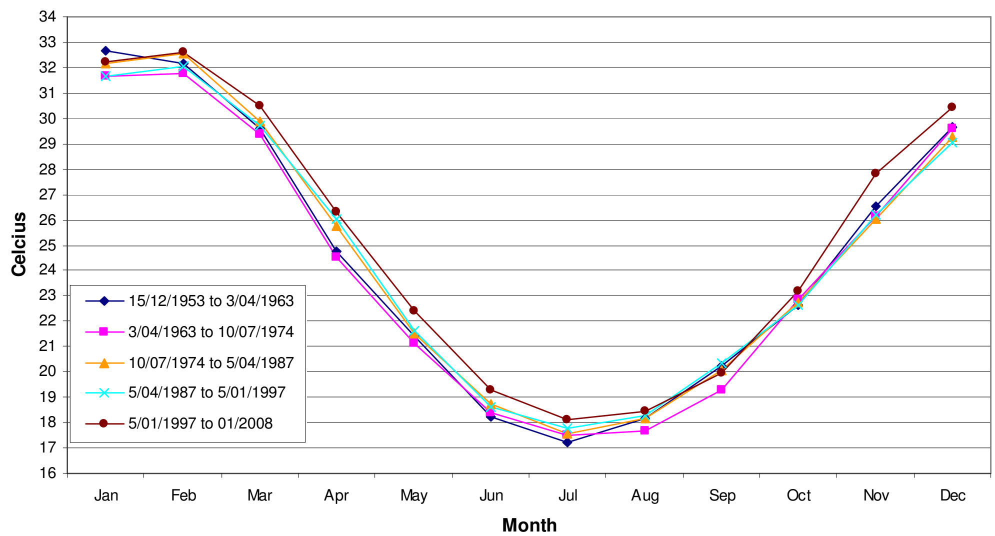

Figure 27: Average monthly maximum temperature per orthophoto epoch at station 9029 located at Muchea tree farm.

In comparison the changes in average monthly maximum temperature over the 55 years are not so great. There has been a slight increase in the early winter (May and June) temperatures in the most recent epoch, shown in Figure 27. No changes in average monthly minimum temperature in each epoch were observed and the data is not presented.

The increase in the rate of spread in the epoch 1992-1997 (Figure 13) indicated the need to examine in more detail the rainfall pattern. Rainfall was extremely high (263.4mm) in June 1991 (Figure 28) compared to the 1987-2007 June average of 130.9mm (Figure 26). In addition the total rainfall for June and July in 1995 and 1996 was greater than 150mm (Figure 28) and higher than the average winter rainfall for this 10 year epoch (Figure 26).

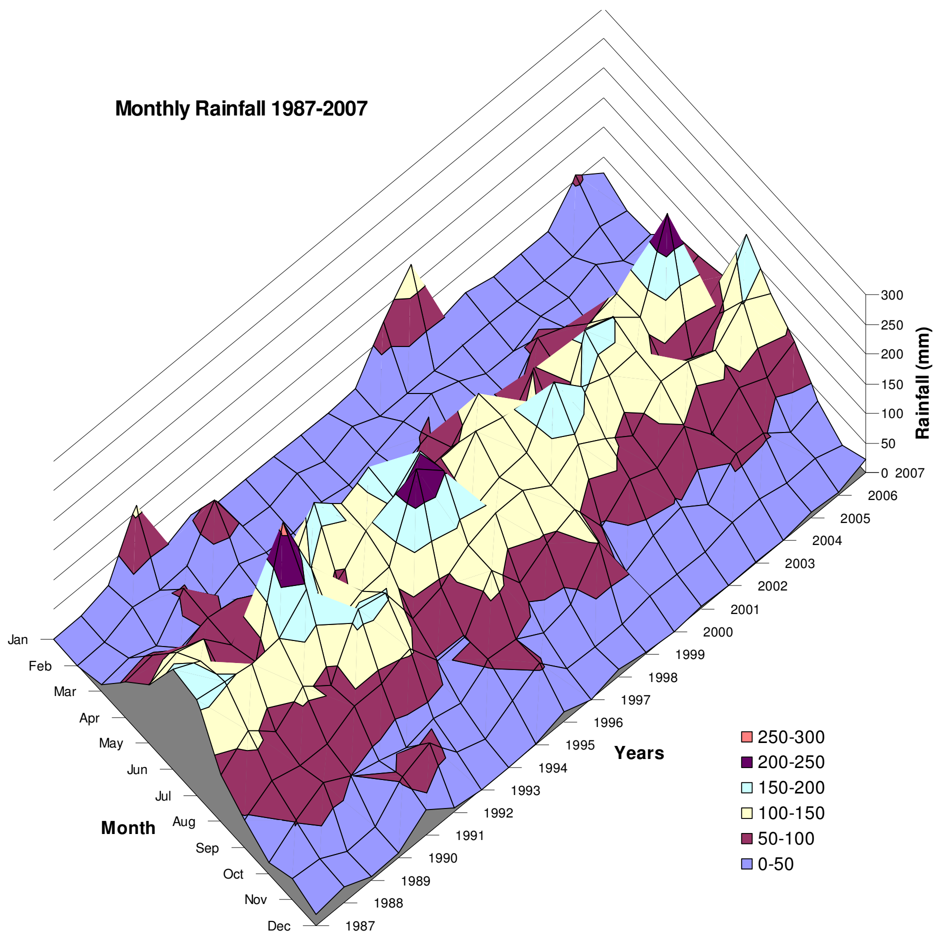

Figure 28: Total monthly rainfall per year 1987 to 2007 at station 9029 located at Muchea tree farm.

Discussion

This study has shown that remote sensing technologies can be used to map the impact of Phytophthora dieback in *Banksia* woodlands. There was a high degree of overlap between areas identified as impacted by the disease from ground based survey methods and remote sensing methods involving a combination of orthophotos interpretation and Landsat Trend information. The boundaries of disease impacted areas did not always align exactly however this is likely to be related to the ability of ground based methods to more effectively discriminate disease impact in all structural layers and on individual plants and of the ground strata in the early stages of infestation. Remote sensing methods, on the other hand, can only detect the disease once it has had a major impact on the vegetation particularly the upper structural layers. On ground assessments are also more likely to differentiate impacts from the pathogen from other threatening processes which are also impacting vegetation. Despite these limitations, the use of remote sensing technologies has a number of benefits. These include (1) the availability of orthophoto and Landsat image archives which enable historical and current mapping of disease impact to be undertaken; (2) can be applied over large areas thus allowing broad scale mapping to be undertaken; (3) no risk of spreading the disease whilst broad scale mapping is being undertaken. Therefore for organisations that have remote sensing capabilities these tools can provide a cost efficient way of identifying disease impact over broad scale areas of *Banksia* woodlands. Once the extent of disease impact is known a risk assessment can be undertaken to prioritise and identify management actions such as more detailed on ground interpretation mapping or actions to protect biodiversity assets such as hygiene measures (if infested), quarantine measures (if un-infested) or phosphite application (Kinloch and Wilson 2009; Kinloch *et al.* 2009b).

Over 55 years the rate of *P. cinnamomi* spread at the Warbrook Road study site was significantly higher in the 1953 – 1963 time interval (1.286m/year) and the lowest rate of spread was recorded for 1997 – 2008 (0.526m/year). The rates of spread between 1953 and 1988 calculated in this study cannot be directly compared to those determined by Hill *et al*. (1994) of 1.36m/year and 0.89m/year) as this current study covered only part of the same study area and different methods were used to calculate spread. However, they are of the same order of magnitude. Another study observed a rate of spread of 1.0m/year on

Banksia woodland at Gnangara (Shearer and Hill 1989) whilst a rate of spread of 1.3 – 1.8m/year has been recorded for western coastal sandplains (Shearer *et al.* 2004). These rates are much less than those recorded for downhill extension in *Banksia* woodland of 8 m/year (Podger 1968), or 400 m / year in sands with an impeding horizon at 1- 8m depth at Wilson's Promontory, Victoria (Weste and Law 1973). Upslope disease extension on the Darling Plateau is 0.37 m/year, compared to 2.15 m/year for the Blackwood Sedimentary Plateau where a perched watertable provides long periods of favourable conditions for proliferation of the pathogen (Strelein *et al.* 2006). In the jarrah forest, upslope and across slope spread seldom exceeds an average of 1 m per year (O'Gara *et al.* 2005). Rates of 0.7- 2m / year have been recorded in the Southern west Botanical province of Western Australia depending on climate, site and susceptibility of vegetation (Grant and Barrett 2003; Hill *et al.* 1994; Shearer *et al.* 2004). The rates recorded in this study at Warbrook Road occur within this range.

At the Warbrook Road study site the area of infestation by the pathogen increased substantially over the 55 years from 14% (65 ha) of the area to 47% (214 ha). A considerable proportion of the area was impacted prior to 1953 and the initial infection is likely to have occurred before 1942 (Hill *et al.* 1994). During subsequent decades the swamp complex at the site became contaminated, initiating disease fronts several kilometres long. Our analysis found that there was a large increase in impacted areas between 1974 and 1988 reflecting the length of the time between dates, and the identification of several new infections in 1988. Further in 1988 there were several discrete disease fronts which have in subsequent years coalesced to form two long fronts in the south-west and north-east of the study area. This demonstrates how *Phytophthora cinnamomi* can spread in an unmanaged susceptible landscape.

Our remote sensing assessment of Warbrook Road and areas such as Pinjar (Figure 8) and Gnangara Pine plantation (Figure 7) show that many initial infestations in the GGS study area begin as small foci and do take time, in some cases decades, to move through the landscape autonomously. However, because the areas are not subject to adequate quarantine or hygiene, vectoring of the pathogen continues its spread across the landscape. The identification of these initial small foci by remote sense methods provides the opportunity to initiate hygiene, treatment and quarantine management to contain or prevent progressive spread of the disease. In the case of threats to biodiversity values it can also highlight potential risks to Threaten Ecological Communities (TECS), listed flora and fauna taxa. Selection of sites for phosphite treatment would also be an option. The phosphite fungicide is an effective treatment in activating host plant defence mechanisms in susceptible plant species and can thus prevent or retard infestation (Cahill *et al.* 2008; Guest and Grant 1991).

The pattern of initial infestation as circular foci indicates that the infestation begins as a spot infection or inoculum. A disease centre is characterised by dead vegetation and a surrounding disease front by recently killed or dying vegetation. The progression of the front is initially by growth of the pathogen through the root systems and the root to root contact. In sites with deep sand the transmission is mainly root to root and as such the radiating foci are common. This differs to other landscapes where long fronts of infestation occur and are often related to surface or subsurface water movement of the pathogen.

Vegetation and landscape factors

There was evidence that the type of vegetation infested affected the rate of spread of *Phytophthora.* Disease impact spread was at a higher rate in J1 vegetation compared to I1. The J1 vegetation (*Banksia, Melaleuca* woodland) occurs more in low lying areas associated with water tables while I1 (Low open *B.attenuata* woodland) occurs more broadly from dune crest to low lying areas making some areas dryer and thus less conducive environment for the pathogen. The dune crest areas are also likely to be infested at a slower rate from upslope progression of the disease (Figure 20).

While initially 50% of the I1 vegetation type was infested, after 1997 I1 this increased to 80-90% (Figure 12a). Only 10% of J1 was infected early on and this increased to only 20-30% post 1997. The area of I1 vegetation type (x ha) was much smaller than the J1 vegetation type (x ha). The areas that remain uninfected are J1 vegetation type and therefore are susceptible, and likely to become infested. The presence of tracks in these areas is likely to contribute to the spread of the disease in these areas also.

A number of landscape factors were also found to have an impact on the rate of spread of the pathogen. The rate of spread of the pathogen was higher in those areas of the landscape where moisture levels are higher and therefore are more conducive to the spread of the pathogen. These landscape characteristics include soil types of humus podzols of poorly drained depressions and areas subject to seasonal inundation. Other areas of deep white and pale yellow sands are interspersed with swamp areas and are subject to seasonal inundation and therefore would generally be wetter. Rate of spread was greater in areas which have a southern aspect and therefore are in shadow for greater periods of time, conditions also conducive to the pathogen (Figure 15, Figure 20 and Figure 21). Rate of spread is also higher in areas with low to mid elevation levels and areas where the groundwater is close to the surface the two variables being not independent (Figure 16, Figure 18, Figure 2).

It was expected that rate of spread would be faster on flat and downhill slopes compared to uphill slopes. However the rate of spread was found to be faster uphill than on the flat and downhill slopes (Figure 22). This maybe related to the fact that in the early epochs, when rate of spread was fastest, the pathogen had already infested the flat and downhill areas of and therefore new uninfected areas available to the pathogen would be above the drainage line. Movement of the pathogen would thus have been uphill onto the surrounding floodplain (Hill *et al.* 1994).

The rate of spread of the pathogen was also higher in those areas of the landscape where elevation change was steep, regardless of direction (Figure 17), and the groundwater was moving either downgrade or upgrade (Figure 19). Dispersal of the pathogen propagules are greatly facilitated by water flowing in surface and near surface drainage systems (Cahill *et al.* 2008; O'Gara *et al.* 2005; Shearer *et al.* 2007b).

There were significant interactions between epoch, vegetation type and depth to water. In vegetation type J1 the pathogen was restricted early on (1953-63), to areas with near surface water, to near surface and shallow water until 1988, and subsequently was present in all depth water categories. In the I1 woodland vegetation, the pathogen was present over a wider range of depth to water categories in the first two epochs and subsequently all depth to water categories. The restriction of the pathogen to more shallow depth to water categories in the early years (Figure 12c) is a reflection of the initially spread of the pathogen along the flank of the floodplain from Sawpit Creek (Hill *et al*. 1994) where depth to water was generally shallower.

There were significant interactions between epoch, vegetation type and elevation change. There were slow rates of spread on flat areas and fast rates of spread on steep uphill or downhill areas continued for the three epochs (1953 – 1988) for both vegetation types. While in the final epoch (1997 – 2008) the rate of spread was much lower and no trend with steepness was evident.

Significant interactions between epoch, vegetation type and slope direction were evident. There was no consistent trend between vegetation type and slope direction in the early epochs (1953– 1988) however subsequently the *Banksia, Melaleuca* vegetation type (J1) generally had a higher rate of spread across all slope directions (Figure 25d and e).

Impact of climate

Examination of rainfall patterns indicated that rainfall may be a major factor influencing the rate of spread with those epochs experiencing higher winter rainfall (1953 – 1963, 1963 – 1974 and 1974 – 1988; Figure 26) having a higher rate of spread across all categories of tested landscape factors (Figure 23 to Figure 25). Rates of spread did decline for the 1988 – 1997 epoch but not substantially, possibly due to a number of wet winters which may have assisted the spread of pathogen for short periods (Figure 23 to Figure 25; Figure 28). The slow rate of spread for all categories of tested landscape factors for the 1997 – 2008 epoch (Figure 23 to Figure 25) occurred when average winter monthly rainfall has declined (Figure 26). Under low rainfall any surface water or near surface drainage transport of the pathogen will decline. Further, host species are likely to suffer from drought stress which may decrease contact between root systems or inhibit lesion growth thereby decreasing the rate of plant to plant spread (Crombie *et al.* 1988; Tippett *et al.* 1987 cited in Hill et al. 1994).

The much lower rate of spread across all depth to water, elevation change, and slope categories in the final epoch (1997 – 2008) may indicate that they only influence rate of spread when winter rainfall is at least average or is greater than average. It is possible that rainfall has an over-riding influence on rate of spread and the influence of landscape variables such as slope, are less influential (Figure 25). Further analyses of rainfall impacts on rate of spread are required. These could include impacts of monthly, annual or winter rainfall on rates of spread within the epochs and any interactions with variables such as vegetation type and slope direction.

Although the increase in temperature in the area was not large it may be significant when coupled with the lower rainfall in the same epoch. The pathogen requires water to multiply and the warmer drier winter conditions would not provide the damp environment the pathogen requires (O'Gara *et al.* 2005). Therefore the slowing of the rate of spread in the last epoch may be influenced by these climatic changes.

Implications of the study

There were some limitations to the current study including the limited verification in the field, especially at the Pinjar site. Another constraint was the availability of data for the investigation of influence of landscape factors on the rate of spread. All combinations of the factors were not available for the early epochs. The DTW (depth to water) information was available only from 2005 and may not be appropriate for earlier epochs or a good quality generalisation for the final epoch. However, sufficient data was available for elevation change and slope landscape factors. Further development of the analysis could employ logistic regression analyses of the variables including rainfall to identify which of the interacting factors may be most predictive (Wilson *et al.* 2000; Wilson *et al.* 2003; Wilson *et al.* 1997).

This study has however greatly improved our assessment of the location of infestation and the rates of spread of Phytophthora dieback in *Banksia* woodlands, and provided information to better inform management of the pathogen on the GGS.

The remote sensed imagery, calibrations and on ground assessments and analyses present quantitative, repeatable methods that can be applied at scales ranging from small remnants to the whole region of the GGS. The analyses can be extended retrospectively and into the future as data is captured on an ongoing basis and it can be employed to provide information for assessing change and monitoring spread.

The results should be employed to implement and maintain hygiene standards for movement of vehicles along the current tracks. Unmapped areas should be considered protectable and be treated with the same hygiene as uninfested areas. Tracks should be demarcated with standardized dieback posts. Options to reduce the impact of *P. cinnamomi* in protectable areas should be considered including application of phosphite, upgrading of tracks that intersect known infestations (e.g. to tracks that do not allow soil movement), particularly tracks traversing wetland and moisture gaining sites and closure of tracks that intersect known infestations.

Other projects undertaken for the GSS have identified the impacts of *P. cinnamomi* on biodiversity assets over the GGS and the risks to them (Kinloch 2009; Swinburn 2009; Swinburn *et al.* 2009). Two threatened ecological communities TECs are considered at high risk, four at moderate and four at low risk (Swinburn 2009). Kinloch (2009) developed multi-criteria evaluation models to rank the biodiversity assets across the GSS study area. The ranking of biodiversity assets is an essential step in the process of formulating conservation priorities alongside identifying the risks that threatening processes pose to these assets. Application of remote sensing methods to assess the presence of infestation or the locality of close infestations should be considered as an important monitoring tool for management of high to moderate risk communities. Implementation of hygiene measures and phosphite application could be then well targeted.

Recommendations for further investigation and management

- Undertake a study of the historic rate of spread and the effects of landscape factors atthe Pinjar site. This site has areas of higher elevation and probably depth to water and the initial infection is more recent. There is one large area of infestation and many small pockets probably infected by movement of vehicles off road. Historic orthophotos have been purchased by the GSS but cannot be done within the GSS timeframes.

- Develop the model further by merging of some categories for some landscape factors, analysing rainfall impacts and developing regression models to resolve the most predictive factors.

- Continue to apply remote sensing methods to monitor rates of spread of the pathogen and assess the efficacy of any management actions undertaken (see below)

- Apply and maintain hygiene standards for movement of vehicles along tracks and demarcate the tracks with standardized dieback signage

- Upgrade tracks that intersect known infestations particularly tracks traversing wetland and moisture gaining sites and close tracks that intersect with known infestations

- Prioritise areas for the application of phosphite to reduce the impact and spread of P. cinnamomi

- Evaluate management actions such as hygiene, quarantine measures, track closures, and application of phosphite employing remote sensing techniques

References

Akashi Y. & Mueller-Dombois D. (1995) A landscape perspective of the Hawaiian rain forest dieback. *Journal of Vegetation Science* **6**, 449-64.

Annett K. (2008) Impacts of the plant pathogen *P. cinnamomi* (Cinnamon fungus) on fauna and ecosystem functions. Deakin University, Melbourne, Australia.

Apan A., Held A., Phinn S. & Markley J. (2004) Detecting sugarcane 'orange rust' disease using EO-1 Hyperion hyperspectral imagery. *International Journal of Remote Sensing* **25**, 489-98.

Austin M. P. (2002) Spatial prediction of species distribution: an interface between ecological theory and statistical modelling. *Ecological Modelling* **157**, 101-18.

Bluett V., Weste G. & Cahill D. M. (2003) Distribution of disease caused by *Phytophthora cinnamomi* in Wilsons Promontory National Park and potential for further impact. *Australasian Plant Pathology* **32**, 479-91.

Caccetta P. A., Campbell N. A., Evans F. H., Furby S. L., Kiiveri H. T. & Wallace J. F. (2000) Mapping and monitoring land use and condition change in the South-West of Western Australia using remote sensing and other data. In: *Proceedings of the Europa 2000 Conference*, Barcelona.

Cahill D. M., Harding C., O'May J. & Wilson B. A. (2002) Assessment of guidelines for best practice management of *Phytophthora cinnamomi* in parks and reserves across Victoria. Parks Victoria, University of Ballarat.

Cahill D. M., Rookes J. E., Wilson B. A., Gibson L. & McDougall K. L. (2008) *Phytophthora cinnamomi* and Australia's biodiversity: impacts, predictions and progress towards control. *Australian Journal of Botany* **56**, 279-310.

Chaerle L. & Van der Straeten D. (2000) Imaging techniques and the early detection of plant stress. *Trends in Plant Science* **5**, 495-501.

Crombie D. S., Tippett J. T. & Hill T. C. J. (1988) Dawn water potential and root depth of trees and understorey species in south-western Australia. *Australian Journal of Botany* **36**, 621-31.

Daniel R., Taylor J. & Guest D. (2006) Distribution and occurrence of *Phytophthora cinnamomi* at Middle Head and North Head, Sydney Harbour. *Australasian Plant Pathology* **35**, 569-71.

DOW. (2008) Gnangara groundwater areas - Water Management Plan (draft for public comment). Department of Water, Perth WA.

Environment Australia. (2009) Threatened Species and Ecological Communities. Australian Government.

Essa S., Dohai B. & Taoufik K. (2006) Mapping dynamics of invasive prosopis juliflora in the northern Emirates of the UAE: and application of remote sensing and GIS. In: *ISPRS Commission VII Mid-term Symposium "Remote Sensing: From Pixels to Processes"* pp. 459-65, Enschede, Netherlands.

Furby S. L., Renzullo L. J., Chia J. & Wallace J. F. (2004) The Use of Spectral Indices and Spatially Varying Threshold Surfaces for Mapping the Extent of Perennial Vegetation over Time. In: *The 12th Annual Australasian Remote Sensing and Photogammetry Conference Proceedings* pp. 18-22, Fremantle, Western Australia.

Furby S. L., Zhu M., Wu X. & Wallace J. (2008) Vegetation Trends 1990-2008 South West Agricultural Region of Western Australia. 2007 Update of the Land Monitor II Project. Product #3 - Vegetation Trends. CSIRO Mathematical and Information Sciences.

Gadek P. A., Gillieson D., Edwards W., Landsber J. & Pryce J. (2001) Rainforest Dieback Mapping and Assessment in the Wet Tropics World Heritage Area. Schools of Tropical Biology, Tropical Environmental Studies, Geography and the Rainforest CRC, James Cook University, Cairns.

Government of Western Australia. (2009) Gnangara Sustainability Strategy - Situation Statement. Department of Water and the Gnangara Sustainability Strategy, Perth, Australia.

Grant M. & Barrett S. (2003) The distribution and impact of *Phytophthora cinnamomi* Rands in the south east coast region of Western Australia. In: *Phytophthora in forests and natural ecosystems. 2nd International IUFRO working party 7.02.09 meeting, Albany, WA.* (eds J. A. McComb, G. E. S. Hardy and I. C. Tommerup). Murdoch University Print, Perth.

Guest D. & Grant B. (1991) The complex action of phosphonates as antifungal agents. *Biological Reviews of the Cambridge Philosophical Society* **66**, 159-87.

Havel J. J. (1968) The potential of the Northern Swan-coastal Plain for *Pinus pinaster* Ait. Plantations. *Bulletin* **76**, 7-73, Forests Department of Western Australia.

Hill R. J., Willson B. A., Rookes J. E. & CaHill D. M. (2009) Use of high resolution digital multi-spectral imagery to assess the distribution of disease caused by *Phytophthora cinnamomi* on heathland in Anglesea, Victoria. *Australasian Plant Pathology* **38**, 110-9.

Hill T. C. J., Tippett J. T. & Shearer B. L. (1994) Invasion of Bassendean Dune Banksia woodland by *Phytophthora cinnamomi*. *Australian Journal of Botany* **42**, 725-38.

Hogg J. & Weste G. (1975) Detection of die-back disease in the Brisbane Ranges by aerial photography. *Australian Journal of Botany* **23**, 775-81.

Kinloch J. (2009) Criteria and ranking of biodiversity assets in the GSS study area. Unpublished report prepared for the Department of Environment and Conservation and the Gnangara Sustainability Strategy, Perth Western Australia.

Kinloch J., Valentine L. E. & Sonneman T. (2009a) Status of Vegetation Complexes in the Gnangara Sustainability Strategy Study Area. Unpublished report prepared for the Department of Environment and Conservation and the Gnangara Sustainability Strategy.

Kinloch J. & Wilson B. (2009) *Phytophthora* dieback risk assessment of Gnangara mound biodiversity assets. Unpublished report for the Department of Environment and Conservation and the Gnangara Sustainability Strategy. Perth.

Kinloch J., Wilson B. & Swinburn M. (2009b) Chapter eleven: Risks and Priorities. In: Biodiversity Values and Threatening Processes of the Gnangara Groundwater System (editors Wilson, B. and Valentine, L.E.). Report prepared for the Gnangara Sustainability Strategy, Perth. http://portal.water.wa.gov.au/portal/page/portal/gss/Content/reports/GSS_BiodiversityValuesAndThreateningProcesses.pdf.

Laidlaw W. S. & Wilson B. A. (2006) Habitat utilisation by small mammals in a coastal heathland exhibiting symptoms of *Phytophthora cinnamomi* infestation. *Wildlife Research* **33**, 639-49.

Lamb D. W. (2000) The use of qualitative airborne multispectral imaging for managing agricultural crops - a case study in south-eastern Australia. *Australian Journal of Experimental Agriculture* **40**, 725-38.

Lenthe J. H., Oerke E. C. & Dhene H. W. (2007) Digital infrared thermography for monitoring canopy health of wheat. *Precision Agriculture* **8**, 15-26.

Liu D., Kelly M. & Gong P. (2006) A spatial-temporal approach to monitoring forest disease spread using multi-temporal high spatial resolution imagery. *Remote Sensing of Environment* **101**, 167-80.

Mattiske Consulting Pty Ltd. (2003) Flora and vegetation studies - Gnangara Mound. Stages 1, 2 and 3. Part A - Report. Report prepared for Water and Rivers Commission and Water Corporation, Perth.

McDougall K. L., Hardy G. E. S. & Hobbs R. J. (2002a) Distribution pf Phytophthora cinnamomi in the northern jarrah (Eucalyptus marginata) forest of Western Australia in releation to dieback age and topography. *Australian Journal of Botany* **50**, 107-14.

McDougall K. L., Hobbs R. J. & Hardy G. E. S. (2002b) Floristic and structural differences between *Phytophthora* infested and adjoining uninfested vegetation in the northern jarrah (*Eucalyptus marginata*) forest of Western Australia. *Australian Journal of Botany* **50**, 277-88.

Metternicht G. (2007) Vegetation indices derived from high-resolution airborne videography for precision crop management. *International Journal of Remote Sensing* **24**, 2855-77.

Mirik M., Michels G. J., Kassymzhanova-Mirik S., Elliot N. C., Catana V., Jones D. B. & Bowling R. (2006) Using digital image analysis and spectral reflectance data to quantify damage by greenbug (Hemiptera: Aphididae) in winter wheat. *Computers and Electronics in Agriculture* **51**, 86-98.

Mitchell D., Williams K. & Desmond A. (2003) Swan Coastal Plain 2 (SWA 2- Swan Coastal Plain Sub-region). In: *A biodiversity audit of Western Australia's 53 Biogeographical subregions in 2002* (eds J. E. May and N. L. McKenzie) pp. 606-23. Department on Conservation and Land Management, Perth, WA.

Newell G. R. & Wilson B. A. (1993) The relationship between cinnamomi fungus (*Phytophthora cinnamomi*) and the abundance of *Antechinus stuartii* (Dasyuridae: Marsupialia) in the Brisbane Ranges, Victoria. *Wildlife Research* **20**, 251-9.

Nilsson H. E. (1995) Remote sensing and image analysis in plant pathology. *Annual Review of Phytopathology* **15**, 489-527.

O'Gara E., Howard K., Wilson B. A. & Hardy G. E. S. J. (2005) Management of *Phytophthora cinnamomi* for Biodiversity Conservation in Australia: Part 2 - National Best Practice Guidelines. In: *A report funded by the Commonwealth Government Department of the Environment and Heritage*. Centre for *Phytophthora* Science and Management, Murdoch University, Western Australia.

Olsson H., Schneider W. & Koukal T. (2008) 3D remote sensing in forestry. *International Journal of Remote Sensing* **29**, 1239-42.

Pickup C., Chewing V. H. & Nelson D. J. (1993) Estimating changes in vegetation over time in arid rangelands using Landsat MSS data. *Remote Sensing of Environment* **43**, 243-63.

Podger F. D. (1968) Aetiology of jarrah dieback and disease of dry sclerophyll *Eucalyptus marginata* Sm. forests in Western Australia. In: *Science*. University of Melbourne, Melbourne.

Podger F. D. & Brown M. J. (1989) Vegetation damage caused by *Phytophthora cinnamomi* on disturbed sites in temperate rainforest in Western Tasmania. *Australian Journal of Botany* **37**, 443-80.

Ristaino J. B. & Gumpertz M. L. (2000) New frontiers in the study of dispersal and spatial analysis of epidemics caused by species in the genus Phytophthora. *Annual Review of Phytopathology* **38**, 541-76.

Shearer B. L., Crane C. E., Barrett S. & Cochrane A. (2007a) Assessment of threatened flora susceptibility to *Phytophthora cinnamomi* by analysis of disease progress curves in shadehouse and natural environments. *Australasian Plant Pathology* **36**, 609-20.

Shearer B. L., Crane C. E., Barrett S. & Cochrane A. (2007b) *Phytophthora cinnamomi* invasion, a major threatening process to conservation of flora diversity in the South-west Botanical Province of Western Australia. *Australian Journal of Botany* **55**, 225-38.

Shearer B. L., Crane C. E. & Cochrane A. (2004) Quantification of the susceptibility of the native flora of the South-West Botanical Province, Western Australia, to *Phytophthora cinnamomi*. *Australian Journal of Botany* **52**, 435-43.

Shearer B. L. & Hill T. C. (1989) Diseases of Banksia woodlands on the Bassendean and Spearwood Dune systems. *Journal of the Royal Society of Western Australia* **71**, 113-4.

Stone C., Old K., Kile G. & Coops N. (2001) Forest health monitoring in Australia: national and regional commitments and operational realities. *Ecosystem Health* **7**, 48-58.

Strelein G. J., Sage L. W. & Blankendaal P. A. (2006) Rate of extension of *Phytophthora cinnamomi* in jarrah forest (*Eucalyptus marginata*) bioregion of south-west Western

Australia. In: *Progress in research on Phyphthora cinnamomi of forest trees. 3rd international IUFRO working party 7.02.09 meeting, Friesing, Germany* (eds C. Braiser, T. Jung and W. Osswald) pp. 49-52. Farnham Forest Research: Surrey, UK, Friesing, Germany.

Swinburn M. (2009) Native plant taxa and threatened ecological communities of the GSS study area: An assessment of susceptibility to *Phytophthora cinnamomi*. Unpublished report prepared by the Department of Environment and Conservation for the Gnangara Sustainability Strategy. Perth.

Swinburn M. L., Valentine L. E., Mickle D. A. & Sonneman T. L. (2009) The impacts of *Phytophthora cinnamomi* on flora and terrestrial fauna on the Gnangara Mound. Unpublished report prepared by the Department of Environment and Conservation for the Gnangara Sustainability Strategy, Perth.

Tchoukanski I. (2008) ET Spatial Techniques. http://www.ian-ko.com/. [Accessed 26/11/2009].

Tippett J. T., Crombie D. S. & Hill T. C. J. (1987) The effect of phloem water relations on the growth of *Phytophthora cinnamomi* in *Eucalyptus marginata. Phytopathology* **77**, 246-50.

Wallace J., Behn G. & Furby S. (2006) Vegetation condition assessment and monitoring from sequences of satellite imagery. *Ecological Management and Restoration* **7**, S31-S6.

Wallace J. F., Canci M., Wu X. & Baddeley A. (2007) Monitoring Native Vegetation on an Urban Groundwater Supply Mound using Airborne Digital Imagery. *Spatial Science.* **52**, 63-73.

Weste G. (1974) *Phytophthora cinnamomi* - the cause of severe disease in certain native communities in Victoria. *Australian Journal of Botany* **29**, 261-76.

Weste G., Brown K., Kennedy J. & Walshe T. (2002) *Phytophthora cinnamomi* infestation - a 24-year study of vegetation change in forests and woodlands of the Grampians, Western Victoria. *Australian Journal of Botany* **50**, 247-74.

Weste G. & Law C. (1973) The invasion of native forest by *Phytophthora cinnamomi:* Threat to the National Park, Wilson's Promontory, Victoria. *Australian Journal of Botany* **21**, 31-51.

Wilson B. A. (1990) The effects of vegetation, fire and other disturbance factors on small mammal ecology and conservation. Ph.D., Deakin University, Geelong.

Wilson B. A., Aberton J. & Cahill D. M. (2000) Relationships between site factors and distribution of *Phytophthora cinnamomi* in the Eastern Otway Ranges, Victoria. *Australian Journal of Botany* **48**, 247-60.

Wilson B. A., Aberton J. & Lewis A. (2003) A spatial model for predicting the presence of cinnamon fungus (*Phytophthora cinnamomi*) in sclerophyll vegetation communities in south-eastern Australia. *Austral Ecology* **28**, 108-15.

Wilson B. A., Lewis A. & Aberton J. (1997) Conservation of national estate communities threatened by cinnamomi fungus at Anglesea, Victoria. Department of Natural Resources and Environment., Melbourne, Victoria.

Zhang M., Qin Z., Liu X. & Ustin S. L. (2003) Detection of stress in tomatoes induced by late blight disease in California, USA, using hyperspectral remote sensing. *International Journal of Applied Earth Observation and Geoinformation* **4**, 295-310.

Appendices

Appendix A: Description of Mattiske Vegetation Types present in study areas.

Taken from Mattiske (2003).

Vegetation Type Code	Description
G1	Low Woodland to Low Open Woodland of *Banksia attenuata - Banksia menziesii - Eucalyptus todtiana - Nuytsia floribunda* with occasional *Allocasuarina fraseriana* and *Banksia grandis* (southern section only) over *Leucopogon conostephioides, Scholtzia involucrata, Eremaea pauciflora* var. *pauciflora, Melaleuca scabra, Boronia purdieana* subsp. *purdieana* and *Astroloma xerophyllum.*
I1	Low Open Woodland of *Banksia attenuata - Banksia menziesii* over *Verticordia nitens, Dasypogon bromeliifolius, Melaleuca seriata* and *Patersonia occidentalis.*
J1	Woodland of *Corymbia calophylla - Banksia attenuata - Banksia menziesii - Melaleuca preissiana* over *Xanthorrhoea preissii, Hypocalymma angustifolium, Pultenaea reticulata, Adenanthos obovatus, Regelia ciliata* and *Jacksonia furcellata.*
K1	Open Forest of *Eucalyptus rudis* subsp. *rudis - Melaleuca preissiana - Banksia ilicifolia* with occasional *Banksia attenuata, Banksia menziesii, Nuytsia floribunda* and *Eucalyptus todtiana* over *Kennedia prostrata, Lyginia barbata, Xanthorrhoea preissii, Hypocalymma angustifolium, Dasypogon bromeliifolius, Pericalymma ellipticum* var. *ellipticum, Astartea scoparia, Lepidosperma tenue, Jacksonia furcellata, Kunzea ericifolia* subsp. *ericifolia* and *Bossiaea eriocarpa.*

Appendix B: Description of Major Soil Types (DAFWA Mapping Units)

Code	**Name**	**Landform Description**	**Soil Description**	**Vegetation Description**
212Bs__Jas	Bassendean, phase Jandakot steep	Jandakot dune ridges. Slopes <15% and usually more than 10m relief.	Grey medium sand overlying pale yellow sands generally underlain by humic and iron podsols.	*Banksia* spp. low open woodland with sparse shrub layer.
212Bs__G	Bassendean, phase G	Flat or gently undulating landscape.	Iron-humus podzols and some diatomite deposits.	*Banksia* spp. Low open woodland with scattered emergent *Eucalyptus calophylla* and *Melaleuca pressiana* dense shrub layer.
212Bs__Ja	Bassendean, phase Jandakot	Jandakot low dunes. Slopes <10% and generally more than 5m relief.	Grey sand over pale yellow sand generally underlain by humic and iron podsols.	*Banksia* spp. low open woodland with a dense shrub layer.
212Bs__J	Bassendean, phase Joel	Poorly drained depressions.	Humus podzols.	Scattered *M. preissiana, E. rudis* and *Banksia ilicifolia* with a dense shrub layer.
212Bs__Ws	Bassendean, phase Ws	Depressions with free water in winter.	Humus podzols and peat.	Dense *M. preissiana; M. rhaphiophylla* and *E. rudis* around the edges with reeds and sedges in the centre.
213Ya_8x	Yanga _8x	Flat plain with occasional low dunes. Subject to seasonal inundation.	Deep white and pale yellow sands interspersed with swamp and generally underlain by siliceous/humic pans at depth.	Low woodland of *E. rudis, Melaleuca* spp., reeds and *Banksia illicifolia*, *B. prionotes, Casuarina* spp. and *E. todtiana* on better drained areas.

Appendix C: Lineal Rate of Spread Epoch Statistics

Rate of spread (m/yr) of pathogen impact over a 55 year time period as calculated by this study (GSS) and over a 35 year time period by Hill *et al*. (1994). The rates are between every available orthophoto date with number of lengths observed (GSS only) .

Epoch	GSS Rate of Spread (m/yr)	GSS Number of observations	Hill *et al.* (1994) Rate of Spread (m/yr)
1953_1963	1.286	753	1.31
1963_1974	1.010	834	1.36
1974_1988	1.180	853	0.89
1988_1992	0.703	1200	N/A
1992_1997	1.080	1121	N/A
1997_2003	0.394	1200	N/A
2003_2008	0.411	1200	N/A

Rate of spread (m/yr) of pathogen impact between orthophoto dates approximately 10 years apart with number of lengths observed.

Epoch	Rate of Spread (m/yr)	Number of observations
1953_1963	1.286	753
1963_1974	1.010	834
1974_1988	1.180	853
1988_1997	0.957	1043
1997_2008	0.526	1174